2023-08-01

# Studies On Atomic And Molecular Properties Using Locally Scaled And Perdew-Zunger Self-Interaction Corrected Density Functional Approximations

Philip Adeniyi Oyedele
*University of Texas at El Paso*

STUDIES ON ATOMIC AND MOLECULAR PROPERTIES USING LOCALLY SCALED AND PERDEW-ZUNGER SELF-INTERACTION CORRECTED DENSITY FUNCTIONAL APPROXIMATIONS

PHILIP A. OYEDELE

Master's Program in Physics

APPROVED:

Rajendra Zope, Ph.D., Chair

Tunnah Baruah, Ph.D.

Mahesh Narayan, Ph.D.

Nair Harikrishnan, Ph.D.

Stephen Crites, Ph.D.
Dean of the Graduate School

*To God; my source and sustainer,*

*To my late mother; for teaching me the ways of the lord,*

*To my Dad; for his sacrifices, love and prayers*

*To everyone instrumental to my growth and progress*

# STUDIES ON ATOMIC AND MOLECULAR PROPERTIES USING LOCALLY SCALED AND PERDEW-ZUNGER SELF-INTERACTION CORRECTED DENSITY FUNCTIONAL APPROXIMATIONS

by

PHILIP A. OYEDELE

THESIS

Presented to the Faculty of the Graduate School of

The University of Texas at El Paso

in Partial Fulfillment

of the Requirements

for the Degree of

MASTER OF SCIENCE

Department of Physics

THE UNIVERSITY OF TEXAS AT EL PASO

August 2023

# Acknowledgement

It is my great pleasure to express my utmost gratitude to my supervisor of this thesis work Dr. Rajendra Zope, it was an extraordinary experience for me to work under his supervision in such a well-equipped lab. His constant guidance, valuable suggestions, encouragement, and innovative ideas was the driving force behind the success of the research work.

I would also like to express my appreciation to my Co-supervisor Dr. Tunna Baruah, for her guidance, thoughtful suggestions, and continuous encouragement throughout the progress of my research work. I also want to appreciate Dr. Selim Romero, Dr. Luis Basurto, and Dr. Yoh Yamamoto for their utmost help, encouragement, critical comments, and cordial dealings throughout the research. I am thankful to my lab mates; Fernando, Prakash, and Pedro for their cooperation and supportive company at the lab and off the lab.

Special appreciation to Mrs. Alero Eyesan Rosaline; your kind words have become a great source of inspiration to me. Thank you for trusting and believing in me.

Adunni Ade, Omolola mi Owon; as I fondly call you, you're indeed a game changer. Thank you for loving me the way you do. 'Amazing' is an understatement to describe you. I can't wait to show you off to the world as mine. Your love hits differently. 'Forever' is the goal.

To my amazing siblings, mentors, and friends who believed in me and helped me pull through this phase of life, y'all are amazing! BSM, FBC El Paso, ISF, and all my El Paso friends and family, you make this journey a great one for me. Thank you!

# Abstract

This thesis examines some properties of atoms and molecules using one-electron self-interaction-correction (SIC) methods such as the Perdew-Zunger SIC (PZSIC) and the locally scaled SIC method of Zope and coworkers within the Fermi-Lowdin SIC formalism. The accuracy of electron density is examined by comparing moments of the density, $\langle r^n \rangle = \int \rho(r) r^n d\tau = \int_0^\infty 4\pi r^2 \rho(r) r^n dr$ $(n = -2, -1, 0, 1, 2, 3)$ with the corresponding available values from the Coupled cluster (CC) singles, doubles, and perturbative triples (CCSD(T)) method. Three test sets are considered: boron through neon neutral atoms, two and four electron cations, and 3d transition metals. Each set was tested with PBE, LDA, PZSIC-PBE, and PZSIC-LSDA functionals using default-NRLMOL basis, aug-cc-pwcvtz, and aug-cc-pwcvqz basis sets. Results show that for the transition metals, PBE and LDA with default basis have smaller deviations compared to PZSIC-PBE and PZSIC-LSDA. The second part of the thesis examines the possibility of obtaining good energetics by perturbatively applying the SIC to the energy using the self-consistent density of various density functionals as well as the Hartree-Fock approximation(s). Such an approach provides significantly improved barrier heights compared to uncorrected DFAs. Our results show that the LSIC method [Zope *et al., J. Chem. Phys.* **151**, 214108 (2019)] consistently performs better than the PZSIC method. This preliminary work suggests such an approach can be useful for certain properties.

**Keywords:Self-interaction error, self-interaction correction, density functionals, electron density, moments of density**

# Table of Contents

# List of Tables

# List of Figures

# Chapter 1

# Density Functional Theory

There are many fields within the physical sciences and engineering where the key to technological progress is understanding and controlling the properties of matter at the level of individual atoms and molecules.

Density functional theory (DFT) in its Kohn-Sham formulation[1] is, an exact theory for describing the ground state properties of matter and offers an attractive alternative to the wave function theory (WFT). An important difference between DFT and WFT is the principal quantity of interest. In DFT, this quantity is the ground state electron density which, unlike the wavefunction, is an observable. The computational advantage of DFT originates from the fact that electron density has three spatial coordinates, regardless of the number of electrons in the chemical system. Thus DFT allows the calculation of structures and properties of molecules with a couple of hundred atoms, a feat not generally possible with high-level WFT methods[2].

### 1.0.1 Atomic Units

To facilitate a more concise, readable mathematical formalism, this manuscript will use *Hatree atomic units*. specifically, we shall set[3]

$$\hbar = e = m_e = a_o = 1 \tag{1.0.1}$$

where $\hbar$ is the reduced plank constant, $e$ the charge of the electron, $a_o$ the Bohr radius and $m_e$ the mass of the electron. occasionally, however, this symbols will be included in equations for clarity[3]

### 1.0.2 The Electronic Structure theory

From the non-relativistic quantum theory, the state of any given system is represented by a time-dependent vector in Hilbert space, $\mid \psi\rangle$. This vector obeys the famous Schrodinger equation

$$\hat{H} \mid \psi\rangle = -\imath\hbar\frac{\partial}{\partial t} \mid \psi\rangle \tag{1.0.2}$$

where $i$ denotes the imaginary unit, $\hbar$ denotes the reduced plank constant, $\frac{\partial}{\partial t}$ denotes the partial time derivatives and $\hat{H}$ denotes the Hamiltonian operator. For the so-called stationary state Schrödinger equation gives:

$$\hat{H} \mid \psi\rangle = E \mid \psi\rangle \tag{1.0.3}$$

Herein $E$ denotes the total energy of the system in the stationary state $\mid \psi\rangle$ [4]. All real atomic systems larger than hydrogen consist of multiple electrons, and all molecular systems include multiple atomic nuclei. Such a system, consisting of M nuclei and N electrons, is described by the many-body Hamiltonian[3]:

$$\hat{H} = -\sum_{A}^{M}\frac{\bigtriangledown_A^2}{2m_A} - \sum_{i}^{N}\frac{\bigtriangledown_i^2}{2m_e} + \frac{1}{2}\sum_{A\neq B}^{M}\frac{Z_A Z_B}{r_{AB}} + \frac{1}{2}\sum_{i\neq j}^{N}\frac{e^2}{r_{ij}} - \sum_{i,A}^{N,M}\frac{eZ_A}{r_{ij}} \tag{1.0.4}$$

$$= T_n + T_e + V_{nn} + V_{ee} + V_{en} \tag{1.0.5}$$

The first two terms of (1.4) are the nuclear and electronic kinetic energies, respectively. The latter three terms are the potential energy of nuclear and electronic repulsion and nuclear-electronic attraction. The wavefunction that describes such a system depends upon the positions of all the nuclei and electrons[3].

Neglecting spin for the moment, the stationary state $\mid \psi\rangle$ can be reformulated as the many-body wave function $\psi\rangle = \psi(\vec{r}_1, ..\vec{r}_N, \vec{R}_1, .., \vec{R}_M)$ The mass of the nuclei is so enormous in comparison to the electron mass $m_e$ that, the nuclei stand still from the electronic

point of view, while the electrons themselves appear to be moving instantaneously from the perspective of the nuclei. This is referred as the Born-Oppenheimer or adiabatic approximation, and it leads to a separation of electron dynamics from nuclear dynamics, introducing the electronic Hamiltonian $\hat{H}_e$ This electronic Hamiltonian is written as[4]

$$\hat{H}_e = \hat{T}_e + \hat{V}_{ee} + \hat{V}_{en} \tag{1.0.6}$$

and the total energy is simply the electronic energy plus the internuclear potential, $E_e + V_{nn}$ As the stationary nuclei still interact with the electrons via Coulomb attraction, $\psi$ still depends parametrically upon the nuclear coordinates $\mathbf{R}$[3]

### 1.0.3 The Hohenberg-Kohn (HK) Theorems

The development of DFT began with the discovery of the HK theorem and according to a widely adopted point of view the HK theorem plays the central role within DFT[5]. The first HK theorem proved in 1964[6] guarantees that the ground state properties of a molecular electronic system can be fully described by the electron density[6].

#### Theorem 1

*For molecules with a nondegenerate ground state, the ground state molecular energy, wavefunction and other electronic properties are uniquely determined by the ground state electron probability density* $\rho_o(r)$ The first HK theorem allows us to write down an expression for the electronic energy as a function of the density.

$$E_o = E[\rho_o] = T[\rho_o] + V_{en}[\rho_o] + V_{ee}[\rho_o] = V_{en}[\rho_o] + F[\rho_o] \tag{1.0.7}$$

The electron-nuclear interaction energy $V_{en}$ is known and determined by the parametric positions of the atomic nuclei. However, the unknown functional F, containing the electron kinetic energy and correlation terms, is unknown and must be approximated. The second

HK theorem provides a variational principle for the ground state energy as a functional of the electron density, and renders the above equation practically applicable.

**Theorem 2**

*The energy as a functional of some trial electron density, $\rho(r) \geq 0$ such that $\int dr\rho(r) = N$, provides an upper bound to the ground state energy.*

$$E_o \leq E[\rho(r)] \tag{1.0.8}$$

*Furthermore, the ground state electron density is that which minimizes the energy functional, and provides the true ground state energy.*

$$E[\rho(r)] = E_o \iff \rho(r) = \rho_o(r) \tag{1.0.9}$$

These two facts allow for the self-consistent calculation of the ground state energy of a molecular system.

### 1.0.4 The Kohn-Sham (KS) Equation

While the HK theorems are powerful formal statements, they must be exploited to create a practical tool for calculating energies. In 1965, Kohn and Sham devised a method for finding $\rho_o$ and then calculating $E_o$[1]. In principle, the method permits an exact solution, however since the unknown functionals $T$ and $V_{ee}$ must be approximated, the solutions are necessarily also approximate.

Kohn and Sham began by considering a reference system, s, consisting of N noninteracting electrons in an external potential $V_s(r)$, whose ground state electron density $\rho_s(r)$ is the same as the true system's ground state density $\rho_o(r)$. The Hamiltonian of the noninteracting system is:

$$H_s = \int_i^N (-\frac{\nabla_i^2}{2} + V_s(r)) = \sum_i^N h_i^{KS} \tag{1.0.10}$$

Furthermore, the noninteracting system's ground state wavefunction can be represented as a Slater determinant of the lowest-energy Kohn-Sham spin orbitals $\psi_i^{KS}$ that are eigenfunctions of the one-electron Hamiltonian.

$$\Psi_o = \mid \psi_1^{KS}, \psi_2^{KS}, ..., \psi_N^{KS} \rangle \tag{1.0.11}$$

$$h_i^{KS}\psi_i^{KS} = \epsilon_i^{KS}\psi_i^{KS} \tag{1.0.12}$$

Kohn and Sham then rewrote (1.10) by considering the deviations of the kinetic and potential energy of the real system from the reference system

$$\triangle T[\rho] = T[\rho] - T_s[\rho] \tag{1.0.13}$$

$$\triangle V_{ee}[\rho] \equiv V_{ee}[\rho] - \frac{1}{2}\iint dr_1 dr_2 \frac{\rho(r_1)\rho(r_2)}{r_{1,2}} \tag{1.0.14}$$

(1.10) can then be written as

$$E[\rho] = T_s[\rho] + V_{en}[\rho] + U[\rho] + E_{XC}[\rho] \tag{1.0.15}$$

where $U[\rho]$ is the classical coulomb potential and introduces the newly defined *exchange-correlation energy* that characterizes the energy associated with electron exchange and correlation effects.

$$E_{XC} \equiv \triangle T[\rho] + \triangle V_{ee}[\rho] \tag{1.0.16}$$

As no exact form of $E_{XC}$ is known, it must be approximated, and doing so is key to accurate DFT calculations, as well as a long-ongoing area of active research. Because the reference system is defined to have the same ground-state electron density as the true system, we may construct a guess (or 'trial') ground-state density as the superposition of

probability densities of the constituent KS wavefunctions.

$$\rho = \rho_s = \sum_{i}^{N} \mid \psi_i^{KS} \mid^2 \tag{1.0.17}$$

Now, in a manner analogous to the HF method, we can vary $\rho$ by varying the KS orbitals $\psi_i^{KS}$ (subject to the constraint that they remain orthogonal) in order to minimize $E_{[\rho]}$. The orbitals that minimize the molecular ground state energy can be shown to satisfy the *Kohn-Sham equations*.

$$(-\frac{\nabla_i^2}{2} + V_{eff}(r)) \mid \psi_i^{KS} = \epsilon_i \mid \psi_i^{KS} \rangle \tag{1.0.18}$$

Thus, we have arrived at a set of N nonlinear equations that can be solved using a selfconsistent variational process akin to the HF method. The Kohn-Sham equations describe the motion of noninteracting electrons in the field of an *effective potential*

$$V_{eff} \equiv V_{en}[\rho] + V_c[\rho] + V_{XC}[\rho] \tag{1.0.19}$$

which captures the effects of the interactions of the electrons with the nuclei and each other. The unknown *exchange-correlation potential* is defined as the functional derivative of the exchange-correlation energy.

$$V_{XC}[\rho] \equiv \frac{\delta E_{XC}[\rho]}{\delta \rho} \tag{1.0.20}$$

*Kohn-Sham density functional theory* is analogous to HF in many ways. However, the principal difference is that where HF depends upon approximating the ground state wavefunctions using a single determinant, the electron density of DFT can be known exactly. Conversely, the effective potential of DFT must be approximated due to the exchange-correlation term. Stated more plainly, HF is an exact theory with an approximate solution, DFT is an approximate theory with an exact solution.

### 1.0.5 Functional for Exchange And Correlation

#### Local Density Approximation LDA

The local spin density approximation[7, 3, 4] LDA was developed by Kohn and Sham and it tells that, for systems where the electron density varies over space the exchange and correlation are primarily local phenomena [7]. for spin- unpolarized homogenous system the exchange energy is analytically as a functional of the density in the LDA approximation[7, 3, 4].

$$E_{xc}[\rho] = \int d^3r \epsilon_{xc}^{LDA}(\rho(r)) \tag{1.0.21}$$

Where $\epsilon_{xc} = \epsilon_x + \epsilon_c$

$\epsilon_{xc}^{LDA}(\rho(r))$ is the exchange energy density that depend on $(\rho(r))$ and is defined as:

$$\epsilon_{xc}^{LDA}(\rho) = -\frac{3^{\frac{3}{4}}}{4\pi^{\frac{1}{3}}}\rho^{\frac{4}{3}} \tag{1.0.22}$$

for spin polarized homogenous system the exchange energy is analytically as a functional of the density in the LDA approximation

$$E_{xc}[\rho^{\uparrow}, \rho^{\downarrow}] = \frac{1}{2}(E_{xc}[2\rho^{\uparrow}] + E_{xc}[2\rho^{\downarrow}]) \tag{1.0.23}$$

LDA gives close to correct exchange-correlation energy to systems that have similar properties to homogenous system like the close shell system, metal, and electron gas[4].

#### Generalized Gradient Approximation, GGA

The generalized gradient approximation[4] exchange-correlation energy is a functional of both the local spin densities and the local spin density gradients[4, 3]. It uses the dimensionless enhancement factor $F(s)$ as

$$E_{xc}^{GGA}[\rho, \bigtriangledown\rho] = \int d^3r \epsilon_{xc}^{LDA}(\rho(r))F_{xc}(s(r)) \tag{1.0.24}$$

where

$$S = \frac{| \bigtriangledown \rho |}{[2(3\pi^2)^{\frac{1}{3}} \rho^{\frac{4}{3}}]} \tag{1.0.25}$$

**Further Exchange-Correlation Approximation**

While LDA represents the simplest form of the exchange-correlation functional, and the one used by the methods discussed in this manuscript, many more sophisticated approximate functionals exist. This area in particular has historically been one of the most active areas of research in DFT. While the mathematical and physical detail of other functionals is beyond the scope of this work, a summary of developments beyond LDA and GGA includes:

*local spin-density approximations* (LSDA), whose construction depends upon separating the up and down spin electron densities [8, 9]

*hybrid functionals*, first proposed by Becke [10] that exploit some exact exchange results from HF theory.

And most recently, *meta-generalized-gradient approximations* that also take into account the kinetic energy density, such as the 'strongly-constrained and appropriately normed' (SCAN) approximation [11].

It can be noted that each functionals possess their characteristic strengths and weaknesses, and their usefulness is heavily dependent on the system at hand[4]. The development of new and better functionals remains one of the main challenges in advancing density functional theory within the Kohn-Sham ansatz[3, 4]. However, instead of creating an entirely original functional, it is often more practical to add a term to those already existing functionals, in order to correct some of their more apparent shortcomings. Many of the corrections currently in use aim to eliminate the so-called self-interaction error (SIE) [12, 4, 7, 13, 14]. The cause of this error and the different approaches to tackle it will be the topic of the following section.

# Chapter 2

# Self-Interaction Corrections to Density Functional Theory

A major problem of solid-state theory and quantum chemistry is to understand the behavior of many electrons interacting via Coulomb's law

$$\hat{V_{ee}} = \frac{1}{2} \sum_{1} \sum_{i \neq j} \frac{1}{\mid \vec{r_i} - \vec{r_j} \mid} \tag{2.0.1}$$

In the earliest quantum-mechanical theory, Thomas and Fermi replaced the expectation value $\langle \hat{V_{ee}} \rangle$ by the direct Coulomb energy, a functional of the electron number density $\rho(r)$ :

$$U[\rho] = \frac{1}{2} \int d^3r \int d^3r' \frac{\rho(\vec{r})\rho(\vec{r'})}{\mid \vec{r} - \vec{r'} \mid} \tag{2.0.2}$$

As early as 1934, Fermi and Amaldi' observed the failure of the above equation to vanish for one-electron systems due to the spurious self-interaction inherent in it, and proposed the first and crudest version of self-interaction correction[14]. Most of the available approximations are semilocal approximations, where the XC energy density at a certain point only depends on the density and derivatives of the density at that point. These approximations have been extensively used thanks to their computational efficiency and they generally work well, but they all contain the self-interaction error (SIE), which means that the sum of the Hartree interaction energy and the approximated XC energy does not properly vanish for all one-electron systems. SIE causes a wide range of problems, such as

the XC potential decaying too fast asymptotically, the orbital energies of occupied orbitals lying too high in a nonsystematic way, and the total energy varying in a strongly nonlinear way between adjacent integer electron numbers[15]

For solids, the SIE has been identified as the cause of the systematic underestimation of the semiconductor band gaps[4]. These gaps are calculated as differences of orbital energy eigenvalues - specifically, as the differences between the HOMO (highest occupied molecular orbital) and the LUMO (lowest unoccupied molecular orbital) energies[7, 13, 4]. In general, uncorrected DFT does not fulfil Koopman's theorem, which identifies the HOMO energy as the negative of the ionization potential and the LUMO energy as the negative of the electron affinity[12, 7, 16]

For example, in neutral systems the long-range behavior of the KohnSham (KS) potential does not reduce to the $-\frac{1}{r}$ form expected from general considerations, this and other SIEs lead to a range of related issues, sometimes referred to as delocalization errors when using DFT approximations to understand chemistry, materials, and physics[16, 4].

Zacks and Zope put it in a more simpler term: for a charge density describing any number of electrons, a given electron will 'see' itself in any interaction it has with the whole density[3]. This is the basics of SIE. Eliminating SIE is thus the aim of self-interaction corrections (SIC) to density functional theory. The SIC methods, proposed by Perdew and Zunger and the approach used by Rajendra Zope[17], Mark Pederson[13] et al will be presented in the following subsections

### 2.0.1 Perdew-Zunger Self Interaction Correction

The problem of self-interaction error which occur in density functional theory such as Rydberg state missing, mis-ordering of states of some systems, incorrect description of stretch bonds, problems with unstable anions due to the fact that the sum of the Hartree interaction energy and the approximated exchange correlation energy does not properly vanish for all one-electron system[4].

To relieve the effects of SIE[17], Perdew and Zunger proposed a self-interaction cor-

rection (SIC) method in 1981 now known as Perdew-Zunger self-interaction correction (PZSIC)[17]. PZSIC seeks to correct SIE by subtracting the self-Coulomb and self-exchange energies on an orbital-by-orbital basis[3].

$$E_{XC}^{PZSIC} = E_{XC} - \sum_i (U[\rho_i] - E_{XC}[\rho_i]) \tag{2.0.3}$$

### 2.0.2 Fermi Lowdin Self-Interaction Correction

For a Perdew-Zunger self-interaction-corrected XC functional to find the true minimum energy in a variational calculation, it has been shown that the molecular orbitals used to construct $\rho$ must satisfy the localization equation[18, 19]

$$\langle \psi_i \mid V_i^{PZSIC} - V_j^{SIC} \mid \psi_i \rangle = 0 \tag{2.0.4}$$

The computational difficulty of satisfying this constraint using KS orbitals led to the development of Fermi-Lowdin SIC (FLO-SIC)[3] which uses a Lowdin-orthogonalized set of Fermi orbitals, that are localized by construction. For a given set of KS orbitals, a Fermi orbital (FO) can be defined at any point in space $a_i$ as

$$F_{i\sigma}(r) = \frac{\sum_j \psi_{j\sigma}^*(a_i)\psi_{j_\sigma}(r)}{\sqrt{\sum_j \mid \psi_{j\sigma}(a_i) \mid^2}} = \frac{\rho_\sigma(a_i, r)}{\sqrt{\rho_\sigma(a_i)}} \tag{2.0.5}$$

where $\sigma$ is the spin index and the point $a_i$ is called the Fermi orbital descriptor (FOD). The FO is constructed by a relatively simple transformation of the KS orbitals, and is essentially the ratio of the one-electron spin density to the square root of the total spin-density.

The principal advantage of the FLO-SIC method over PZSIC is its computational efficiency. Optimizing a set of N FOs requires optimizing $3N$ FODs, compared to the $N^2$ parameters that must be optimized to satisfy the localization equation (2.4) with normal KS orbitals.

### 2.0.3 The Paradox of SIC and Local-Scaling SIC

A curious side effect of SIC-DFT calculations is the appearance of the so-called paradox of SIC, in which SIC tends to improve the accuracy of some energetic predictions, while degrading others. In particular, SIC-DFT tends to worsen equilibrium molecular properties of molecules and solids such as atomization energies and equilbrium geometries, and this degradation of accuracy only increases as a DFT calculation climbs Jacob's ladder and SIC is applied to semilocal and hybrid XC functionals. On the other hand, SIC-DFT performs well for nonequilibrium geometries such as stretched molecular bonds.

In 2019, Zope and coworkers were able to partially resolve the paradox by implementing a more selective SIC referred to as local-scaling SIC (LSIC) [19]. Fundamentally, LSIC corrects SIE in the same orbital wise fashion as PZSIC:

$$E_{XC}^{LSIC-DFA} = E_{XC}^{DFA}[\rho_\uparrow, \rho_\downarrow] - \sum_i (U^{LSIC}[\rho_{i\sigma}] - E_{XC}^{LSIC}[\rho_{i\sigma,O}]) \tag{2.0.6}$$

However, the correction is scaled throughout space in such a way that it is only applied in regimes where it is actually needed[19].

$$U^{LSIC}[\rho_{i\sigma}] = \frac{1}{2} \iint dr_1 dr_2 \frac{(z_\sigma(r_1))^k \rho_{i\sigma}(r_1)\rho_{i\sigma}(r_2)}{r_{12}} \tag{2.0.7}$$

$$E_{XC}^{LSIC}[\rho_{i\sigma,0}] = \int dr (Z_\sigma(r_1))^k \rho_{i\sigma}(r) \epsilon_{XC}^{DFA}([\rho_{i\sigma,0}], r) \tag{2.0.8}$$

The titular local-scaling comes in the form of the factor $z_\sigma$ which is defined as the ratio of the von Weizsacker kinetic energy density and the Kohn-Sham kinetic energy density[3].

$$z_\sigma \equiv \frac{\tau_\sigma^W(r)}{\tau_\sigma(r)} \tag{2.0.9}$$

The noninteracting (Kohn-Sham) kinetic energy density is given as

$$\tau_\sigma(r) = \frac{1}{2}\sum_i \mid \bigtriangledown\psi_{i\sigma}(r) \mid^2 \tag{2.0.10}$$

and the von Weiszacker kinetic energy density is the single-orbital limit of $\tau_\sigma(r)$

$$\tau_\sigma^W(r) = \frac{\mid \bigtriangledown\rho_{i\sigma}(r) \mid^2}{8\rho_\sigma(r)} \tag{2.0.11}$$

By definition, $z_\sigma \epsilon [0,1]$, where $z_\sigma = 0$ corresponds to uniform densities, and $z_\sigma = 1$ to one-electron densities. For this reason, $z_\sigma$ is called an iso-orbital indicator, as it detects single-orbital regions of the electron density. The exponent $k$ is a tunable parameter. In particular, $k = 0$ disables the scaling completely and recovers the PZSIC limit, while $k \to \infty$ reduces to a standard DFA by zeroing out SIC entirely. The simplest choice of $k = 1$ interpolates smoothly between the uniform density and one-electron limits.

# Chapter 3

# Accuracy of PZSIC and Kohn-Sham Density

The success of Kohn-Sham (KS) density functional theory (DFT) depends upon three[20], inter-related quantities: the functional ($E_{XC}$), the potential ($V_{XC}$), usually defined as the functional derivative, and the density represented by the first n-KS orbitals, $\rho(x_1) = \sum_i \mid \psi_i \mid^2$ generated by the selfconsistent potential. If all are exact, then so is the total ground state energy. The functionals can be reasonably accurate for many problems, but the potential is more sensitive to a correct description of exchange and correlation; and if that potential is not accurate, then the orbitals to construct the density will not be either[20].

Although density functional theory (DFT)is one of the important methods for the study of the electronic structures of molecules,[21] it is difficult to improve the approximations and corrections embedded therein[22, 23, 24]. We have previously suggested that an accurate representation of the electron density can serve as the basis for the development of functionals for use in DFT[23]. The advantage of this approach is that the electron density is a scalar quantity covering all space and can thus provide much more information than integrated quantities such as the total energy. Also, the electron density is more sensitive to the errors introduced by the use of an approximate wave function than the total energy. An accurate density will in general, result in good values for the energy as well as other related quantities, whereas a low energy does not have to be associated with an accurate total density[22, 23].

Kohn–Sham density functional theory (KS-DFT)[25] has been very successful for calculating energetic quantities like reaction energies and barrier heights and for calculating

geometries of molecules and lattice constants of solids.[25] A question that has been less well studied is, how accurate are the electron densities that it predicts?[26].

Pragya Verma and Donald G. Truhlar[26] said the first nonzero moment of the charge density of a neutral molecule is its dipole moment[27], and so – before one considers more detailed characteristics of charge distributions – it is important to first examine how well KS-DFT can predict that leading moment[26, 27]. Furthermore, an exchange-correlation functional that leads to an accurate representation of the charge distribution of a molecule should accurately predict the dipole moments of the molecule[26]

It is well known that Kohn–Sham density functional theory (DFT) is more accurate for the energetics of single-reference systems than for the energetics of multi-reference ones[26], but there has been less study of charge distributions. Verma in his work benchmarked 48 density functionals using organic and inorganic molecules, all the 48 methods tested here were found to give good performance for single-reference molecules. For other multi-reference molecules, functionals with high HF exchange or high local exchange were found to give large errors. He concluded that there is not a lot of difference in the ability of various density functionals to represent the first moment of the electron density. Furthermore, all density functionals he tested so far are considerably better for charge distributions of single-reference molecules than for charge distributions of multireference molecules[26].

Xuefei Xu et al[28] concluded in their work that conventional CC methods including CCSD-(T), CCSDT, and CCSDT(2)Q have performance (judged by comparison to available experimental data) only comparable to, but not necessarily better than KS density functional calculations with a wide set of choices of xc functionals, and they cannot be assumed to provide validated benchmarks for KS theory.[28].

### 3.0.1 Expectation Values of Densities

The correctness of the density is a logical figure of merit in electronic structure theory and is the objective for this contribution. One can view the KS-DFT equations as an approximation to a correlated orbital theory[29, 30] (COT) whose effective one-particle equations

contain a potential for electron correlation, along with the kinetic energy and exchange contributions and the classical coulomb interaction $h_x = \hat{t} + \hat{v} + \hat{J} + \hat{V}_x + \hat{V}_c = \hat{t} + \hat{V}_s$. In KS-DFT as long as the energy functional is convex, it should provide an energy that is correct to the second order in $\rho(r)$. However, the potential $V_s(r) = \frac{\partial E}{\partial \rho(r)}$, used to generate the orbitals in the Kohn–Sham (KS) determinant is only accurate to the first order in $\rho(r)$ This raises concern about the accuracy of the potential [30]. Modern day KS-DFT calculations pay little attention to the accuracy of the $V_{xc}$, and consequently, the orbitals and the density $\rho(r)$ they define can suffer. Construction of many density functionals is semi-empirically adjusted to produce accurate total energy properties, particularly, thermochemistry. Recent publications by Medvedev *et al* [31] and Brorsen *et al* [32] suggest that after the year 2000, there is a decrease in the accuracy of the density produced by such modern semiempirical functionals. in other words, recent functional development has strayed from the path of better approximations to the exact functional. The recent study of Medvedev *et al* [31] used "normalized" maximum errors, or root mean square deviation of the density, gradient of the density, and Laplacian of the density of beryllium through neon neutral atoms and cations to rank the density functionals compared to coupled cluster singles and doubles (CCSD).[31, 30, 33] A similar analysis by Kallay *et al* recently used a composite coupled cluster (CC) singles, doubles, triples, and quadruples (CCSDTQ) as reference density for some atoms and a small collection of molecules.[34] Brorsen *et al* [32] argue that many atoms in the study of Medvedev et al. are positively charged and the bulk of the density is localized in core regions which can cancel in a reaction. Therefore, the accuracy of the electron density near the valence region is deemed more important and in this work, the density of interest is the all-electron (core + valence) density.

There are several differences in the present study on the accuracy of densities compared to previous publications. [31, 32, 34, 35, 36, 37] First, the reference for the correct density is CCSD(T) which can be readily evaluated for essentially any system of interest. Why CCSD(T)? Couple Cluster (CC) theory is usually considered to be the most accurate and most powerful electronic structure method that is applicable to moderate-sized molecules,

and it has been successfully applied for the prediction and in-depth understanding of chemical structure, properties, reactivity, and mechanisms[28]. CC theory becomes exact as one includes successively higher and higher excitation operators (double, triple, quadruple, ...), but for many complex systems, CC calculations are not affordable (although recent advances are changing this situation dramatically), and even when such calculations are affordable, one is often limited to double excitations with a quasi-perturbative treatment of connected triple excitations. However, this theory, called CCSD(T)[38], is very successful and has even been called the "gold standard" of quantum chemistry[38, 28]. The trust in CCSD(T) calculations is so high that, in the absence of experimental data, CCSD(T) results are frequently used as reference values (also called benchmark values) of chemical properties; for example, CCSD(T) calculations are often used for validation of the accuracy of other theoretical methods, such as KS methods [39, 28]

Second, the study includes $3d$ transition metals. Third, instead of taking pointwise differences on a grid relative to a reference density to evaluate the accuracy of a method, following, Schweigert *et al* [40] the difference is assessed by computing the expectation value of $r^n$, $\langle r^n \rangle$ where $r$ is the distance from the nucleus and $n = -2, -1, 0, 1, 2, 3$. The performance of PBE functional is compared to PZIC PBE and PZSIC LSDA while CCSD(T) as reference.

$$\langle r^n \rangle = \int \rho(r) r^n d\tau = \int_0^\infty 4\pi r^2 \rho(r) r^n dr \tag{3.0.1}$$

The $\langle r^n \rangle$ moments of the density can be interpreted as representing different regions in space, particularly, the short- and long-range behavior of the density $\rho(r)$ The values $n < 0$ weigh more toward emphasizing the core region and the values $n > 0$ weigh the valence region of the density.

Density functional approximations PBE[41], and LDA[41] are considered in this study along with PZSIC PBE[42] and PZSIC LSDA[42]. The focus of this work is to study and assess the accuracy of PZSIC densities.

In this work, we consider three test sets. The first test set consists of neutral atoms:

B, C, N, O, F, and Ne. The second test set consists of cations with 2 and 4 electrons: $B^{+}$, $C^{2+}$, $N^{3+}$, $O^{4+}$, $F^{5+}$, $Ne^{6+}$, $B^{3+}$, $C^{4+}$, $N^{5+}$, $O^{6+}$, $F^{7+}$, and $Ne^{8+}$. The third test set consists of the neutral ground state transition metals Sc, Ti, V, Cr, Mn, Fe, Co, Ni, Cu, and Zn. The summary is in the table below:

Table 3.1: Test Sets for Calculation of Expectation values

| Test Sets | Systems |
|---|---|
| $Set1$ | $B$, $C$, $N$, $O$, $F$, and $Ne$. |
| $Set2a$ | $B^{+}$, $C^{2+}$, $N^{3+}$, $O^{4+}$, $F^{5+}$, and $Ne^{6+}$. |
| $Set2b$ | $B^{3+}$, $C^{4+}$, $N^{5+}$, $O^{6+}$, $F^{7+}$, and $Ne^{8+}$. |
| $Set3$ | $Sc$, $Ti$, $V$, $Cr$, $Mn$, $Fe$, $Co$, $Ni$, $Cu$, and $Zn$. |

For the three sets, the DEFAULT-NRLMOL basis, aug-cc-pwCVQZ[30], and aug-cc-pwCVTZ[30] basis sets were used for the calculations. The KS-DFT calculations are performed with the NRLMOL program package. One assumes that CCSD(T) calculations provide the best reference density[38, 28]. Hence, the deviation of $\langle r^n \rangle$ compared to results from CCSD(T)[38] is one measure of the accuracy of the density. Another is the comparison to the radial distribution functions themselves.

For the purpose of brevity to avoid long tables, the basis set will be represented with symbols

Table 3.2: Basis Sets representation

| Basis Sets | Symbols |
|---|---|
| Default Basis | a |
| Aug-cc-pwcvqz | b |
| Aug-cc-pwcvtz | c |

The result obtained are presented in the following tables

Table 3.3: Expectation values of Set1 with DFA-PBE

| System | Basis | $R^{-2}$ | $R^{-1}$ | $R^0$ | $R^1$ | $R^2$ | $R^3$ | $CCSD(T)R^{-1}$ | $\%ErrR^{-1}$ |
|---|---|---|---|---|---|---|---|---|---|
| Ne | a | 415.2076 | 31.0916 | 10.0000 | 8.0027 | 9.8302 | 15.9557 | 31.1036 | 0.04 |
| | b | 415.1240 | 31.0881 | 10.0000 | 8.0043 | 9.8406 | 16.0382 | 31.1036 | 0.05 |
| | c | 414.7148 | 31.0829 | 10.0000 | 8.0059 | 9.8467 | 16.0631 | 31.1036 | 0.07 |
| F | a | 331.3192 | 26.5030 | 9.0000 | 7.8846 | 10.7323 | 19.2835 | 26.5131 | 0.04 |
| | b | 331.2609 | 26.5014 | 9.0000 | 7.8847 | 10.7394 | 19.3773 | 26.5131 | 0.04 |
| | c | 330.8505 | 26.4939 | 9.0000 | 7.8894 | 10.7609 | 19.4916 | 26.5131 | 0.07 |
| O | a | 257.4288 | 22.2472 | 8.0000 | 7.7101 | 11.7004 | 23.3446 | 22.2580 | 0.05 |
| | b | 257.4336 | 22.2447 | 8.0000 | 7.7139 | 11.7262 | 23.5447 | 22.2580 | 0.06 |
| | c | 256.7026 | 22.1714 | 8.0000 | 7.8349 | 12.2475 | 25.7300 | 22.2580 | 0.39 |
| Ni | a | 193.4038 | 18.3254 | 7.0000 | 7.4334 | 12.5745 | 27.6240 | 18.3400 | 0.08 |
| | c | 193.1533 | 18.3218 | 7.0000 | 7.4373 | 12.6079 | 27.9206 | 18.3400 | 0.10 |
| | b | 193.3915 | 18.3248 | 7.0000 | 7.4356 | 12.5943 | 27.7990 | 18.3400 | 0.08 |
| C | a | 138.9391 | 14.6862 | 6.0000 | 7.1918 | 14.1685 | 36.2147 | 14.6988 | 0.09 |
| | b | 138.9483 | 14.6859 | 6.0000 | 7.1966 | 14.2166 | 36.6409 | 14.6988 | 0.09 |
| | c | 138.7929 | 14.6839 | 6.0000 | 7.1984 | 14.2296 | 36.7553 | 14.6988 | 0.10 |
| B | a | 93.8111 | 11.3800 | 5.0000 | 6.8051 | 15.9524 | 48.6200 | 11.3936 | 0.12 |
| | b | 93.8174 | 11.3777 | 5.0000 | 6.8191 | 16.0665 | 49.5507 | 11.3936 | 0.14 |
| | c | 93.7053 | 11.3784 | 5.0000 | 6.8115 | 16.0219 | 49.3384 | 11.3935 | 0.13 |

Table 3.4: Expectation values of Set1 with PZSIC-LSDA

| System | Basis | $R^{-2}$ | $R^{-1}$ | $R^0$ | $R^1$ | $R^2$ | $R^3$ | $CCSD(T)R^{-1}$ | $\%ErrR^{-1}$ |
|---|---|---|---|---|---|---|---|---|---|
| Ne | a | 414.4972 | 31.1788 | 10.0000 | 7.8455 | 9.2743 | 14.1812 | 31.1036 | -0.24 |
| | c | 414.6949 | 31.1846 | 10.0000 | 7.8456 | 9.2761 | 14.1887 | 31.1036 | -0.26 |
| | b | 414.6853 | 31.1842 | 10.0000 | 7.8457 | 9.2762 | 14.1888 | 31.1035 | -0.26 |
| F | a | 330.9344 | 26.5866 | 9.0000 | 7.7173 | 10.0833 | 17.0047 | 26.5130 | -0.28 |
| | c | 330.9344 | 26.5867 | 9.0000 | 7.7173 | 10.0833 | 17.0047 | 26.513 | -0.28 |
| | b | 330.9344 | 26.5867 | 9.0000 | 7.7173 | 10.0833 | 17.0047 | 26.5131 | -0.28 |
| O | a | 257.1392 | 22.3209 | 8.0000 | 7.5404 | 10.9793 | 20.5734 | 22.2580 | -0.28 |
| | c | 257.1392 | 22.3209 | 8.0000 | 7.5404 | 10.9793 | 20.5734 | 22.2580 | -0.28 |
| | b | 257.1392 | 22.3209 | 8.0000 | 7.5404 | 10.9793 | 20.5734 | 22.2580 | -0.28 |
| Ni | a | 193.1799 | 18.3875 | 7.0000 | 7.2796 | 11.8741 | 24.7318 | 18.3400 | -0.26 |
| | c | 193.1799 | 18.3875 | 7.0000 | 7.2796 | 11.8741 | 24.7318 | 18.3400 | -0.26 |
| | b | 193.1799 | 18.3875 | 7.0000 | 7.2796 | 11.8741 | 24.7318 | 18.3400 | -0.26 |
| C | a | 138.7408 | 14.7383 | 6.0000 | 7.0309 | 13.3369 | 32.3302 | 14.6988 | -0.27 |
| | c | 138.7281 | 14.7367 | 6.0000 | 7.0329 | 13.3451 | 32.3608 | 14.6988 | -0.26 |
| | b | 138.7366 | 14.7379 | 6.0000 | 7.0312 | 13.3381 | 32.3346 | 14.6988 | -0.27 |
| B | a | 93.6941 | 11.4223 | 5.0000 | 6.6481 | 15.0063 | 43.4250 | 11.3936 | -0.25 |
| | c | 93.6941 | 11.4223 | 5.0000 | 6.6481 | 15.0063 | 43.4250 | 11.3936 | -0.25 |
| | b | 93.6941 | 11.4222 | 5.0000 | 6.6481 | 15.0063 | 43.4250 | 11.3936 | -0.25 |

Table 3.5: Expectation values of Set1 with PZSIC-PBE

| System | Basis | $R^{-2}$ | $R^{-1}$ | $R^0$ | $R^1$ | $R^2$ | $R^3$ | $CCSD(T)R^{-1}$ | $\%ErrR^{-1}$ |
|---|---|---|---|---|---|---|---|---|---|
| Ne | a | 414.4821 | 31.0987 | 10.0000 | 7.9006 | 9.4067 | 14.4952 | 31.1036 | 0.02 |
| | c | 414.4821 | 31.0987 | 10.0000 | 7.9006 | 9.4067 | 14.4952 | 31.1036 | 0.02 |
| | b | 414.4821 | 31.0987 | 10.0000 | 7.9006 | 9.4067 | 14.4952 | 31.1035 | 0.02 |
| F | a | 330.7770 | 26.5156 | 9.0000 | 7.7740 | 10.2309 | 17.3786 | 26.5131 | -0.01 |
| | c | 330.5322 | 26.5006 | 9.0000 | 7.7810 | 10.2493 | 17.4246 | 26.5130 | 0.05 |
| | b | 330.7770 | 26.5155 | 9.0000 | 7.7740 | 10.2309 | 17.3786 | 26.5130 | -0.01 |
| O | a | 257.0186 | 22.2629 | 8.0000 | 7.5991 | 11.1461 | 21.0209 | 22.2581 | -0.02 |
| | c | 257.0186 | 22.2628 | 8.0000 | 7.5991 | 11.1461 | 21.0209 | 22.2580 | -0.02 |
| | b | 257.0186 | 22.2628 | 8.0000 | 7.5991 | 11.1461 | 21.0208 | 22.2580 | -0.02 |
| Ni | a | 193.1077 | 18.3384 | 7.0000 | 7.3486 | 12.1012 | 25.4340 | 18.3400 | 0.01 |
| | c | 193.1077 | 18.3384 | 7.0000 | 7.3486 | 12.1012 | 25.4340 | 18.3400 | 0.01 |
| | b | 193.1077 | 18.3384 | 7.0000 | 7.3486 | 12.1012 | 25.4341 | 18.3400 | 0.01 |
| C | a | 138.6218 | 14.7018 | 6.0000 | 7.1015 | 13.6071 | 33.2729 | 14.6988 | -0.02 |
| | c | 138.6218 | 14.7018 | 6.0000 | 7.1015 | 13.6071 | 33.2729 | 14.6988 | -0.02 |
| | b | 138.6218 | 14.7018 | 6.0000 | 7.1015 | 13.6071 | 33.2729 | 14.6988 | -0.02 |
| B | a | 93.5775 | 11.3988 | 5.0000 | 6.7142 | 15.3098 | 44.6656 | 11.3936 | -0.05 |
| | c | 93.5775 | 11.3988 | 5.0000 | 6.7142 | 15.3098 | 44.6656 | 11.3936 | -0.05 |
| | b | 93.5774 | 11.3988 | 5.0000 | 6.7142 | 15.3098 | 44.6656 | 11.3936 | -0.05 |

Table 3.6: Expectation values of Set1 with DFA-LDA using default basis

| System | $R^{-2}$ | $R^{-1}$ | $R^0$ | $R^1$ | $R^2$ | $R^3$ | $CCSD(T)R^{-1}$ | $\%ErrR^{-1}$ |
|---|---|---|---|---|---|---|---|---|
| B | 92.44263 | 11.30304 | 5.0000 | 6.83934 | 16.11308 | 49.30866 | 11.39359 | 0.79 |
| C | 137.18534 | 14.60756 | 6.0000 | 7.20961 | 14.22438 | 36.33558 | 14.6988 | 0.62 |
| Ni | 191.26562 | 18.24564 | 7.0000 | 7.44698 | 12.60774 | 27.64547 | 18.34004 | 0.51 |
| O | 254.92965 | 22.15974 | 8.0000 | 7.72765 | 11.74121 | 23.38411 | 22.25804 | 0.44 |
| F | 328.40300 | 26.41291 | 9.0000 | 7.89565 | 10.74284 | 19.21651 | 26.51308 | 0.38 |
| Ne | 411.87457 | 30.99827 | 10.0000 | 8.01488 | 9.84766 | 15.93488 | 31.10355 | 0.34 |

Table 3.7: Expectation values of Set2a with PZSIC-PBE

| System | Basis | $R^{-2}$ | $R^{-1}$ | $R^0$ | $R^1$ | $R^2$ | $R^3$ | $CCSD(T)R^{-1}$ | $\%ErrR^{-1}$ |
|---|---|---|---|---|---|---|---|---|---|
| $Ne^{6+}$ | a | 411.6825 | 23.4370 | 4.0000 | 1.7315 | 1.2432 | 1.1249 | 23.4396 | 0.01 |
| | c | 410.9172 | 23.4361 | 4.0000 | 1.7313 | 1.2429 | 1.1243 | 23.4395 | 0.01 |
| | b | 411.1184 | 23.4368 | 4.0000 | 1.7312 | 1.2428 | 1.1239 | 23.4395 | 0.01 |
| $F^{5+}$ | a | 330.1928 | 20.9378 | 4.0000 | 1.9596 | 1.6001 | 1.6483 | 20.9391 | 0.01 |
| | c | 329.4766 | 20.9367 | 4.0000 | 1.9591 | 1.5995 | 1.6470 | 20.9391 | 0.01 |
| | b | 329.7693 | 20.9395 | 4.0000 | 1.9587 | 1.5984 | 1.6449 | 20.9391 | 0.00 |
| $O^{4+}$ | a | 257.5334 | 18.4376 | 4.0000 | 2.2577 | 2.1377 | 2.5568 | 18.4385 | 0.01 |
| | c | 256.9906 | 18.4358 | 4.0000 | 2.2573 | 2.1374 | 2.5560 | 18.4385 | 0.01 |
| | b | 257.3152 | 18.4388 | 4.0000 | 2.2568 | 2.1359 | 2.5531 | 18.4385 | 0.00 |
| $N^{3+}$ | a | 193.9979 | 15.9359 | 4.0000 | 2.6654 | 3.0064 | 4.2906 | 15.9377 | 0.01 |
| | c | 193.7032 | 15.9361 | 4.0000 | 2.6647 | 3.0051 | 4.2884 | 15.9376 | 0.01 |
| | b | 193.8599 | 15.9364 | 4.0000 | 2.6649 | 3.0059 | 4.2897 | 15.9377 | 0.01 |
| $C^{2+}$ | a | 139.4451 | 13.4343 | 4.0000 | 3.2578 | 4.5522 | 8.0703 | 13.4363 | 0.01 |
| | c | 139.3757 | 13.4368 | 4.0000 | 3.2559 | 4.5461 | 8.0527 | 13.4363 | 0.00 |
| | b | 139.4437 | 13.4359 | 4.0000 | 3.2568 | 4.5491 | 8.0613 | 13.4363 | 0.00 |
| $B^{+}$ | a | 94.0207 | 10.9320 | 4.0000 | 4.2069 | 7.7588 | 18.2395 | 10.9335 | 0.01 |
| | c | 93.7966 | 10.9176 | 4.0000 | 4.2209 | 7.8145 | 18.4344 | 10.9335 | 0.15 |
| | b | 94.0171 | 10.9326 | 4.0000 | 4.2073 | 7.7616 | 18.2474 | 10.9335 | 0.01 |

Table 3.8: Expectation values of Set2a with DFA-PBE using Default basis

| System | $R^{-2}$ | $R^{-1}$ | $R^0$ | $R^1$ | $R^2$ | $R^3$ | $CCSD(T)R^{-1}$ | $\%ErrR^{-1}$ |
|---|---|---|---|---|---|---|---|---|
| $B^{+}$ | 94.18063 | 10.91566 | 4.0000 | 4.21903 | 7.80540 | 18.44864 | 10.93351 | 0.16 |
| $C^{2+}$ | 139.60964 | 13.41853 | 4.0000 | 3.26378 | 4.56779 | 8.12222 | 13.43626 | 0.13 |
| $N^{3+}$ | 194.05954 | 15.91899 | 4.0000 | 2.66950 | 3.01513 | 4.31337 | 15.93769 | 0.12 |
| $O^{4+}$ | 257.48357 | 18.41881 | 4.0000 | 2.26110 | 2.14386 | 2.56971 | 18.43854 | 0.11 |
| $F^{5+}$ | 330.03506 | 20.92033 | 4.0000 | 1.96203 | 1.60398 | 1.65549 | 20.93912 | 0.09 |
| $Ne^{6+}$ | 411.52590 | 23.42062 | 4.0000 | 1.73340 | 1.24583 | 1.12930 | 23.43957 | 0.08 |

Table 3.9: Expectation values of Set2a with DFA-LDA using default basis

| System | $R^{-2}$ | $R^{-1}$ | $R^0$ | $R^1$ | $R^2$ | $R^3$ | $CCSD(T)R^{-1}$ | $\%ErrR^{-1}$ |
|---|---|---|---|---|---|---|---|---|
| $Ne^{6+}$ | 408.49864 | 23.33769 | 4.0000 | 1.73779 | 1.25151 | 1.13626 | 23.43957 | 0.43 |
| $F^{5+}$ | 327.37272 | 20.83857 | 4.0000 | 1.96781 | 1.61267 | 1.66785 | 20.93912 | 0.48 |
| $O^{4+}$ | 255.15316 | 18.33898 | 4.0000 | 2.26806 | 2.15602 | 2.58988 | 18.43854 | 0.54 |
| $N^{3+}$ | 192.06153 | 15.84014 | 4.0000 | 2.67974 | 3.03725 | 4.35866 | 15.93769 | 0.61 |
| $C^{2+}$ | 137.92229 | 13.34111 | 4.0000 | 3.27761 | 4.60475 | 8.21717 | 13.43626 | 0.71 |
| $B^{+}$ | 92.83974 | 10.84138 | 4.0000 | 4.24007 | 7.88137 | 18.71346 | 10.93351 | 0.84 |

Table 3.10: Expectation values of Set2a with PZSIC-LSDA

| System | Basis | $R^{-2}$ | $R^{-1}$ | $R^0$ | $R^1$ | $R^2$ | $R^3$ | $CCSD(T)R^{-1}$ | $\%ErrR^{-1}$ |
|---|---|---|---|---|---|---|---|---|---|
| $Ne^{6+}$ | a | 411.7987 | 23.4472 | 4.0000 | 1.7274 | 1.2366 | 1.1161 | 23.4396 | -0.03 |
| | c | 411.7988 | 23.4472 | 4.0000 | 1.7274 | 1.2366 | 1.1161 | 23.4396 | -0.03 |
| | b | 411.7988 | 23.4471 | 4.0000 | 1.7274 | 1.2365 | 1.1160 | 23.4395 | -0.03 |
| $F^{5+}$ | a | 330.2977 | 20.9481 | 4.0000 | 1.9542 | 1.5903 | 1.6335 | 20.9391 | -0.04 |
| | c | 330.2962 | 20.9480 | 4.0000 | 1.9542 | 1.5903 | 1.6335 | 20.9391 | -0.04 |
| | b | 330.2813 | 20.9474 | 4.0000 | 1.9544 | 1.5906 | 1.6338 | 20.9391 | -0.04 |
| $O^{4+}$ | a | 257.6707 | 18.4487 | 4.0000 | 2.2505 | 2.1228 | 2.5308 | 18.4385 | -0.06 |
| | c | 257.5747 | 18.4437 | 4.0000 | 2.2518 | 2.1255 | 2.5354 | 18.4385 | -0.03 |
| | b | 257.5468 | 18.4422 | 4.0000 | 2.2522 | 2.1262 | 2.5368 | 18.4385 | -0.02 |
| $N^{3+}$ | a | 194.1737 | 15.9494 | 4.0000 | 2.6548 | 2.9805 | 4.2373 | 15.9377 | -0.07 |
| | c | 194.1796 | 15.9498 | 4.0000 | 2.6546 | 2.9802 | 4.2366 | 15.9377 | -0.08 |
| | b | 194.1795 | 15.9498 | 4.0000 | 2.6546 | 2.9802 | 4.2366 | 15.9377 | -0.08 |
| $C^{2+}$ | a | 139.6544 | 13.4508 | 4.0000 | 3.2405 | 4.5003 | 7.9382 | 13.4363 | -0.11 |
| | c | 139.6543 | 13.4508 | 4.0000 | 3.2405 | 4.5003 | 7.9382 | 13.4363 | -0.11 |
| | b | 139.6545 | 13.4507 | 4.0000 | 3.2405 | 4.5003 | 7.9382 | 13.4363 | -0.11 |
| $B^{+}$ | a | 94.0161 | 10.9318 | 4.0000 | 4.1945 | 7.7116 | 18.0988 | 10.9335 | 0.02 |
| | c | 94.0160 | 10.9317 | 4.0000 | 4.1945 | 7.7116 | 18.0989 | 10.9335 | 0.02 |
| | b | 94.0161 | 10.9318 | 4.0000 | 4.1946 | 7.7116 | 18.0989 | 10.9335 | 0.02 |

Table 3.11: Expectation values of Set2b with PZSIC-PBE

| System | Basis | $R^{-2}$ | $R^{-1}$ | $R^0$ | $R^1$ | $R^2$ | $R^3$ | $CCSD(T)R^{-1}$ | $\%ErrR^{-1}$ |
|---|---|---|---|---|---|---|---|---|---|
| $Ne^{8+}$ | a | 379.1373 | 19.3768 | 2.0000 | 0.3119 | 6.5E-02 | 1.7E-02 | 19.3745 | -0.01 |
| | c | 378.3279 | 19.3747 | 2.0000 | 0.3117 | 6.5E-02 | 1.7E-02 | 19.3745 | 0.00 |
| | b | 378.4985 | 19.3749 | 2.0000 | 0.3116 | 6.5E-02 | 1.7E-02 | 19.3745 | 0.00 |
| $F^{7+}$ | a | 305.2221 | 17.3769 | 2.0000 | 0.3480 | 8.1E-02 | 2.4E-02 | 17.3745 | -0.01 |
| | c | 304.5079 | 17.3745 | 2.0000 | 0.3478 | 8.1E-02 | 2.4E-02 | 17.3745 | 0.00 |
| | b | 304.6874 | 17.3749 | 2.0000 | 0.3478 | 8.1E-02 | 2.4E-02 | 17.3745 | 0.00 |
| $O^{6+}$ | a | 239.1462 | 15.3763 | 2.0000 | 0.3935 | 1.0E-01 | 3.4E-02 | 15.3745 | -0.01 |
| | c | 238.6204 | 15.3738 | 2.0000 | 0.3935 | 1.0E-01 | 3.4E-02 | 15.3745 | 0.01 |
| | b | 238.8772 | 15.3750 | 2.0000 | 0.3934 | 1.0E-01 | 3.4E-02 | 15.3745 | 0.00 |
| $N^{5+}$ | a | 181.2291 | 13.3759 | 2.0000 | 0.4529 | 1.4E-01 | 5.3E-02 | 13.3745 | -0.01 |
| | c | 180.8993 | 13.3742 | 2.0000 | 0.4529 | 1.4E-01 | 5.3E-02 | 13.3745 | 0.00 |
| | b | 181.0631 | 13.3751 | 2.0000 | 0.4528 | 1.4E-01 | 5.3E-02 | 13.3745 | 0.00 |
| $C^{4+}$ | a | 131.2909 | 11.3752 | 2.0000 | 0.5334 | 1.9E-01 | 8.6E-02 | 11.3746 | -0.01 |
| | c | 131.1588 | 11.3747 | 2.0000 | 0.5334 | 1.9E-01 | 8.6E-02 | 11.3746 | 0.00 |
| | b | 131.2488 | 11.3752 | 2.0000 | 0.5334 | 1.9E-01 | 8.6E-02 | 11.3745 | -0.01 |
| $B^{3+}$ | a | 89.4641 | 9.3753 | 2.0000 | 0.6488 | 2.8E-01 | 1.6E-01 | 9.3746 | -0.01 |
| | c | 89.3750 | 9.3749 | 2.0000 | 0.6487 | 2.8E-01 | 1.6E-01 | 9.3746 | 0.00 |
| | b | 89.4321 | 9.3753 | 2.0000 | 0.6487 | 2.8E-01 | 1.6E-01 | 9.3746 | -0.01 |

Table 3.12: Expectation values of Set2b with PZSIC-LSDA

| System | Basis | $R^{-2}$ | $R^{-1}$ | $R^0$ | $R^1$ | $R^2$ | $R^3$ | $CCSD(T)R^{-1}$ | $\%ErrR^{-1}$ |
|---|---|---|---|---|---|---|---|---|---|
| $Ne^{8+}$ | a | 379.2531 | 19.3795 | 2.0000 | 0.3118 | 6.5E-02 | 1.7E-02 | 19.3745 | -0.03 |
| | c | 378.4549 | 19.3775 | 2.0000 | 0.3117 | 6.5E-02 | 1.7E-02 | 19.3745 | -0.02 |
| | b | 378.6281 | 19.3775 | 2.0000 | 0.31166 | 6.5E-02 | 1.7E-02 | 19.37453 | -0.02 |
| $F^{7+}$ | a | 305.3365 | 17.3799 | 2.0000 | 0.3479 | 8.1E-02 | 2.4E-02 | 17.37452 | -0.03 |
| | c | 305.3365 | 17.3799 | 2.0000 | 0.3479 | 8.1E-02 | 2.4E-02 | 17.37452 | -0.03 |
| | b | 305.3365 | 17.3799 | 2.0000 | 0.3479 | 8.1E-02 | 2.4E-02 | 17.3745 | -0.03 |
| $O^{6+}$ | a | 239.2618 | 15.3796 | 2.0000 | 0.3935 | 1.0E-01 | 3.4E-02 | 15.3745 | -0.03 |
| | c | 239.2618 | 15.3796 | 2.0000 | 0.3935 | 1.0E-01 | 3.4E-02 | 15.3745 | -0.03 |
| | b | 239.26176 | 15.3796 | 2.0000 | 0.3935 | 1.0E-01 | 3.4E-02 | 15.3745 | -0.03 |
| $N^{5+}$ | a | 181.3462 | 13.3797 | 2.0000 | 0.4528 | 1.4E-01 | 5.3E-02 | 13.3745 | -0.04 |
| | c | 181.3462 | 13.3797 | 2.0000 | 0.4528 | 1.4E-01 | 5.3E-02 | 13.3745 | -0.04 |
| | b | 181.3462 | 13.3797 | 2.0000 | 0.4528 | 1.4E-01 | 5.3E-02 | 13.3745 | -0.04 |
| $C^{4+}$ | a | 131.4104 | 11.3796 | 2.0000 | 0.5333 | 1.9E-01 | 8.6E-02 | 11.3745 | -0.04 |
| | c | 131.4104 | 11.3796 | 2.0000 | 0.5332 | 1.9E-01 | 8.6E-02 | 11.3745 | -0.04 |
| | b | 131.4104 | 11.3796 | 2.0000 | 0.5332 | 1.9E-01 | 8.6E-02 | 11.3745 | -0.04 |
| $B^{3+}$ | a | 89.5808 | 9.3805 | 2.0000 | 0.6485 | 2.8E-01 | 1.6E-01 | 9.3746 | -0.06 |
| | c | 89.5808 | 9.3805 | 2.0000 | 0.6486 | 2.8E-01 | 1.6E-01 | 9.3746 | -0.06 |
| | b | 89.5808 | 9.3805 | 2.0000 | 0.6486 | 2.8E-01 | 1.6E-01 | 9.3746 | -0.06 |

Table 3.13: Expectation values of Set2b with DFA-PBE using default basis

| System | $R^{-2}$ | $R^{-1}$ | $R^0$ | $R^1$ | $R^2$ | $R^3$ | $CCSD(T)R^{-1}$ | $\%ErrR^{-1}$ |
|---|---|---|---|---|---|---|---|---|
| $B^{3+}$ | 89.64855 | 9.36231 | 2.0000 | 0.65313 | 0.28877 | 1.6E-01 | 9.37463 | 0.13 |
| $C^{4+}$ | 131.48918 | 11.36190 | 2.0000 | 0.53632 | 0.19417 | 8.9E-02 | 11.37455 | 0.11 |
| $N^{5+}$ | 181.33980 | 13.36063 | 2.0000 | 0.45499 | 0.13947 | 5.4E-02 | 13.37454 | 0.10 |
| $O^{6+}$ | 239.22201 | 15.36112 | 2.0000 | 0.39505 | 0.10499 | 3.5E-02 | 15.37453 | 0.09 |
| $F^{7+}$ | 305.21201 | 17.36152 | 2.0000 | 0.34912 | 0.08190 | 2.4E-02 | 17.37452 | 0.07 |
| $Ne^{8+}$ | 379.12317 | 19.36147 | 2.0000 | 0.31274 | 0.06567 | 1.7E-02 | 19.37453 | 0.07 |

Table 3.14: Expectation values of Set2b with DFA-LDA using default basis

| System | $R^{-2}$ | $R^{-1}$ | $R^0$ | $R^1$ | $R^2$ | $R^3$ | $CCSD(T)R^{-1}$ | $\%ErrR^{-1}$ |
|---|---|---|---|---|---|---|---|---|
| $B^{3+}$ | 88.36397 | 9.29693 | 2.0000 | 0.65722 | 0.29212 | 1.6E-01 | 9.37463 | 0.83 |
| $C^{4+}$ | 129.89416 | 11.29503 | 2.0000 | 0.53913 | 0.19604 | 9.0E-02 | 11.37455 | 0.70 |
| $N^{5+}$ | 179.47524 | 13.29393 | 2.0000 | 0.45701 | 0.14061 | 5.4E-02 | 13.37454 | 0.60 |
| $O^{6+}$ | 237.05225 | 15.29315 | 2.0000 | 0.39662 | 0.10576 | 3.5E-02 | 15.37453 | 0.53 |
| $F^{7+}$ | 302.75298 | 17.29307 | 2.0000 | 0.35037 | 0.08244 | 2.4E-02 | 17.37452 | 0.47 |
| $Ne^{8+}$ | 376.35939 | 19.29250 | 2.0000 | 0.31375 | 0.06606 | 1.7E-02 | 19.37453 | 0.42 |

Table 3.15: Expectation values of Set3 with PZSIC-LSDA

| System | Basis | $R^{-2}$ | $R^{-1}$ | $R^0$ | $R^1$ | $R^2$ | $R^3$ | $CCSD(T)R^{-1}$ | $\%ErrR^{-1}$ |
|---|---|---|---|---|---|---|---|---|---|
| Sc | a | 2032.000 | 85.825 | 21 | 20.720 | 47.678 | 179.295 | 85.699 | -0.15 |
| | c | 2032.020 | 85.829 | 21 | 20.706 | 47.573 | 178.593 | 85.699 | -0.15 |
| | b | 2032.020 | 85.829 | 21 | 20.706 | 47.573 | 178.593 | 85.699 | -0.15 |
| Ti | a | 2241.523 | 91.593 | 22 | 20.637 | 44.039 | 156.078 | 91.407 | -0.20 |
| | c | 2241.518 | 91.596 | 22 | 20.624 | 43.964 | 155.662 | 91.407 | -0.21 |
| | b | 2241.463 | 91.822 | 22 | 19.684 | 38.573 | 127.599 | 91.407 | -0.45 |
| V | a | 2461.582 | 97.549 | 23 | 20.269 | 39.462 | 131.990 | 97.258 | -0.30 |
| | c | 2461.651 | 97.538 | 23 | 20.322 | 39.699 | 132.701 | 97.258 | -0.29 |
| | b | 2461.682 | 97.572 | 23 | 20.221 | 39.183 | 130.279 | 97.258 | -0.32 |
| Cr | a | 2692.784 | 103.578 | 24 | 20.084 | 34.843 | 99.223 | 103.422 | -0.15 |
| | c | 2692.784 | 103.578 | 24 | 20.084 | 34.843 | 99.223 | 103.422 | -0.15 |
| | b | 2692.784 | 103.578 | 24 | 20.084 | 34.843 | 99.223 | 103.422 | -0.15 |
| Mn | a | 2935.884 | 109.964 | 25 | 19.756 | 31.254 | 80.305 | 109.389 | -0.53 |
| | c | 2935.884 | 109.964 | 25 | 19.756 | 31.254 | 80.305 | 109.389 | -0.53 |
| | b | 2935.884 | 109.964 | 25 | 19.756 | 31.254 | 80.305 | 109.389 | -0.53 |
| Fe | a | 3188.137 | 115.889 | 26 | 20.896 | 35.304 | 99.074 | 115.628 | -0.23 |
| | c | 3188.138 | 115.889 | 26 | 20.896 | 35.304 | 99.077 | 115.628 | -0.23 |
| | b | 3188.138 | 115.889 | 26 | 20.896 | 35.304 | 99.078 | 115.628 | -0.23 |
| Co | a | 3450.992 | 122.428 | 27 | 20.450 | 31.294 | 79.936 | 122.018 | -0.34 |
| | c | 3450.956 | 122.425 | 27 | 20.448 | 31.277 | 79.870 | 122.018 | -0.33 |
| | b | 3450.928 | 122.410 | 27 | 20.477 | 31.398 | 80.344 | 122.018 | -0.32 |
| Ni | a | 3725.204 | 128.965 | 28 | 20.557 | 30.300 | 75.055 | 128.547 | -0.33 |
| | c | 3724.968 | 128.993 | 28 | 20.523 | 30.155 | 74.502 | 128.547 | -0.35 |
| | b | 3725.199 | 128.963 | 28 | 20.561 | 30.316 | 75.117 | 128.547 | -0.32 |
| Cu | a | 4010.271 | 135.663 | 29 | 20.625 | 29.330 | 70.977 | 135.414 | -0.18 |
| | c | 4010.271 | 135.663 | 29 | 20.625 | 29.330 | 70.977 | 135.414 | -0.18 |
| | b | 4010.271 | 135.663 | 29 | 20.625 | 29.330 | 70.977 | 135.414 | -0.18 |
| Zn | a | 4308.055 | 142.243 | 30 | 21.578 | 32.332 | 81.967 | 142.025 | -0.15 |
| | c | 4308.055 | 142.243 | 30 | 21.578 | 32.332 | 81.967 | 142.025 | -0.15 |
| | b | 4308.055 | 142.243 | 30 | 21.578 | 32.332 | 81.967 | 142.025 | -0.15 |

Table 3.16: Expectation values of Set3 with PZSIC-PBE

| System | Basis | $R^{-2}$ | $R^{-1}$ | $R^0$ | $R^1$ | $R^2$ | $R^3$ | $CCSD(T)R^{-1}$ | $\%ErrR^{-1}$ |
|---|---|---|---|---|---|---|---|---|---|
| Sc | a | 2031.4243 | 85.7365 | 21 | 20.9839 | 49.5224 | 191.3557 | 85.6988 | -0.04 |
| | c | 2031.4243 | 85.7365 | 21 | 20.9839 | 49.5224 | 191.3558 | 85.6988 | -0.04 |
| | b | 2031.4082 | 85.7319 | 21 | 21.0003 | 49.6221 | 191.8949 | 85.6988 | -0.04 |
| Ti | a | 2241.0106 | 91.4842 | 22 | 20.9523 | 46.0684 | 168.4126 | 91.4069 | -0.08 |
| | c | 2241.0110 | 91.4842 | 22 | 20.9526 | 46.0701 | 168.4210 | 91.4069 | -0.08 |
| | b | 2241.0106 | 91.4842 | 22 | 20.9523 | 46.0684 | 168.4126 | 91.4069 | -0.08 |
| V | a | 2460.8400 | 97.4415 | 23 | 20.5076 | 41.0574 | 142.6302 | 97.2585 | -0.19 |
| | c | 2461.1457 | 97.4096 | 23 | 20.7003 | 41.8888 | 144.5877 | 97.2585 | -0.16 |
| | b | 2461.1457 | 97.4096 | 23 | 20.7003 | 41.8886 | 144.5865 | 97.2585 | -0.16 |
| Cr | a | 2691.9919 | 103.4631 | 24 | 20.2604 | 35.7787 | 104.4324 | 103.4223 | -0.04 |
| | c | 2691.9919 | 103.4631 | 24 | 20.2604 | 35.7787 | 104.4324 | 103.4223 | -0.04 |
| | b | 2691.9919 | 103.4631 | 24 | 20.2604 | 35.7787 | 104.4324 | 103.4223 | -0.04 |
| Mn | a | 2935.1003 | 109.9089 | 25 | 19.7733 | 31.3712 | 81.3798 | 109.3886 | -0.48 |
| | c | 2935.1003 | 109.9089 | 25 | 19.7733 | 31.3712 | 81.3798 | 109.3886 | -0.48 |
| | b | 2935.1003 | 109.9089 | 25 | 19.7733 | 31.3712 | 81.3798 | 109.3886 | -0.48 |
| Fe | a | 3187.3592 | 115.7360 | 26 | 21.2629 | 37.3786 | 110.1839 | 115.6285 | -0.09 |
| | c | 3187.3197 | 115.7407 | 26 | 21.2271 | 37.1411 | 108.8063 | 115.6285 | -0.10 |
| | b | 3187.3592 | 115.7360 | 26 | 21.2629 | 37.3784 | 110.1833 | 115.6285 | -0.09 |
| Co | a | 3449.9215 | 122.2790 | 27 | 20.6697 | 32.4123 | 85.7759 | 122.0179 | -0.21 |
| | c | 3449.9135 | 122.2632 | 27 | 20.6997 | 32.5344 | 86.2101 | 122.0179 | -0.20 |
| | b | 3450.4630 | 122.1559 | 27 | 21.2756 | 35.7565 | 102.2015 | 122.0179 | -0.11 |
| Ni | a | 3724.0448 | 128.8197 | 28 | 20.7414 | 31.2255 | 79.9014 | 128.5468 | -0.21 |
| | c | 3724.0389 | 128.8301 | 28 | 20.7233 | 31.1599 | 79.6954 | 128.5468 | -0.22 |
| | b | 3724.0073 | 128.8170 | 28 | 20.7446 | 31.2452 | 80.0205 | 128.5468 | -0.21 |
| Cu | a | 4009.0005 | 135.5151 | 29 | 20.7921 | 30.1634 | 75.3807 | 135.4143 | -0.07 |
| | c | 4009.0005 | 135.5151 | 29 | 20.7921 | 30.1634 | 75.3807 | 135.4143 | -0.07 |
| | b | 4009.0005 | 135.5151 | 29 | 20.7921 | 30.1634 | 75.3807 | 135.4143 | -0.07 |
| Zn | a | 4306.6779 | 142.0925 | 30 | 21.7657 | 33.2731 | 86.6628 | 142.0253 | -0.05 |
| | c | 4306.6779 | 142.0925 | 30 | 21.7657 | 33.2731 | 86.6628 | 142.0253 | -0.05 |
| | b | 4306.6779 | 142.0925 | 30 | 21.7657 | 33.2731 | 86.6628 | 142.0253 | -0.05 |

Table 3.17: Expectation values of Set3 with DFA-PBE using default basis

| System | $R^{-2}$ | $R^{-1}$ | $R^0$ | $R^1$ | $R^2$ | $R^3$ | $CCSD(T)R^{-1}$ | $\%ErrR^{-1}$ |
|---|---|---|---|---|---|---|---|---|
| Sc | 2032.4042 | 85.7299 | 21 | 21.0087 | 49.0622 | 184.9691 | 85.6988 | 0 |
| Ti | 2241.9595 | 91.4416 | 22 | 21.1042 | 46.0529 | 162.6741 | 91.4069 | -0.04 |
| V | 2462.2491 | 97.3118 | 23 | 21.1378 | 43.4441 | 146.3514 | 97.2585 | -0.05 |
| Cr | 2692.3519 | 103.4387 | 24 | 20.7285 | 39.2733 | 126.7591 | 103.4223 | -0.02 |
| Mn | 2935.8261 | 109.3710 | 25 | 21.6259 | 41.0492 | 127.8818 | 109.3886 | 0.02 |
| Fe | 3187.7345 | 115.7053 | 26 | 21.2420 | 36.8158 | 105.5405 | 115.6285 | -0.07 |
| Co | 3450.8013 | 122.1410 | 27 | 21.1017 | 34.1761 | 91.6548 | 122.0179 | -0.10 |
| Ni | 3724.8204 | 128.6775 | 28 | 21.1180 | 32.6041 | 83.6792 | 128.5468 | -0.10 |
| Cu | 4009.7536 | 135.3693 | 29 | 21.1573 | 31.4709 | 78.9512 | 135.4143 | 0.03 |
| Zn | 4307.3830 | 141.9877 | 30 | 21.9013 | 33.4212 | 85.3913 | 142.0253 | 0.03 |

Table 3.18: Expectation values of Set3 with DFA-LDA using default basis

| System | $R^{-2}$ | $R^{-1}$ | $R^0$ | $R^1$ | $R^2$ | $R^3$ | $CCSD(T)R^{-1}$ | $\%ErrR^{-1}$ |
|---|---|---|---|---|---|---|---|---|
| Sc | 2026.9378 | 85.6144 | 21 | 21.1323 | 49.6067 | 186.6034 | 85.6988 | 0 |
| Ti | 2236.6114 | 91.3472 | 22 | 21.1208 | 46.0425 | 162.0352 | 91.4069 | 0.07 |
| V | 2456.7819 | 97.1848 | 23 | 21.2271 | 43.8276 | 147.8891 | 97.25847 | 0.08 |
| Cr | 2687.4422 | 103.2990 | 24 | 20.8762 | 39.7900 | 127.8245 | 103.4223 | 0.12 |
| Mn | 2930.4356 | 109.2858 | 25 | 21.5859 | 40.6331 | 124.8207 | 109.3886 | 0.09 |
| Fe | 3182.4814 | 115.7050 | 26 | 21.0270 | 35.6005 | 99.0260 | 115.6285 | -0.07 |
| Co | 3445.2653 | 122.0570 | 27 | 21.0822 | 33.9404 | 89.8916 | 122.0178 | -0.03 |
| Ni | 3719.1515 | 128.6179 | 28 | 21.0263 | 32.0039 | 80.2297 | 128.5468 | -0.06 |
| Cu | 4004.0955 | 135.2899 | 29 | 21.1243 | 31.1697 | 76.9437 | 135.4143 | 0.09 |
| Zn | 4301.4832 | 141.9053 | 30 | 21.8653 | 33.1049 | 83.3837 | 142.0253 | 0.08 |

### 3.0.2 Results And Discussion

By comparing $\langle r^{-1} \rangle$ to the CCSD(T) value, the performance of different systems with corresponding Basis sets and functionals for $\langle r^{-1} \rangle$ in set1 through to set3 are represented using the Mean absolute error (MAE) in table 3.19, 3.20, 3.21, and 3.22 below

Table 3.19: MAE of $\langle r^{-1} \rangle$ for Set1

| Data Sets | Functionals | Basis Set | $\langle r^{-1} \rangle$ MAE |
|---|---|---|---|
| **Set 1** | **DFA-PBE** | default | 0.0123 |
| | | cc-pwcvtz | 0.0291 |
| | | cc-pwcvqz | 0.0141 |
| **Set 1** | **PZSIC LSDA** | Default | 0.0545 |
| | | cc-pwcvtz | 0.0552 |
| | | cc-pwcvqz | 0.0554 |
| **Set 1** | **PZSIC PBE** | Default | 0.0037 |
| | | cc-pwcvtz | 0.0054 |
| | | cc-pwcvqz | 0.0037 |
| **Set 1** | **DFA-LDA** | Default | 0.0967 |

Table 3.20: MAE of $\langle r^{-1} \rangle$ for Set2a

| Data Sets | Functionals | Basis Set | $\langle r^{-1} \rangle$ MAE |
|---|---|---|---|
| **Set 2a** | **PZSIC LSDA** | Default | 0.0091 |
| | | cc-pwcvtz | 0.0083 |
| | | cc-pwcvqz | 0.0080 |
| **Set 2a** | **PZSIC PBE** | Default | 0.0017 |
| | | cc-pwcvtz | 0.0044 |
| | | cc-pwcvqz | 0.0009 |
| **Set 2a** | **DFA-PBE** | Default | 0.0186 |
| **Set 2a** | **DFA-LDA** | Default | 0.0978 |

Table 3.21: MAE of $\langle r^{-1} \rangle$ for Set2b

| Data Sets | Functionals | Basis Set | $\langle r^{-1} \rangle$ MAE |
|---|---|---|---|
| **Set 2b** | **PZSIC LSDA** | Default | 0.0052 |
| | | cc-pwcvtz | 0.0049 |
| | | cc-pwcvqz | 0.0050 |
| **Set 2b** | **PZSIC PBE** | Default | 0.0015 |
| | | cc-pwcvtz | 0.0003 |
| | | cc-pwcvqz | 0.0006 |
| **Set 2b** | **DFA-PBE** | Default | 0.0131 |
| **Set 2b** | **DFA-LDA** | Default | 0.0804 |

Table 3.22: MAE of $\langle r^{-1} \rangle$ for Set3

| Data Sets | Functionals | Basis Set | $\langle r^{-1} \rangle$ MAE |
|---|---|---|---|
| **Set 3** | **PZSIC LSDA** | Default | 0.2891 |
| | | cc-pwcvtz | 0.2911 |
| | | cc-pwcvqz | 0.3125 |
| **Set 3** | **PZSIC PBE** | Default | 0.1669 |
| | | cc-pwcvtz | 0.1636 |
| | | cc-pwcvqz | 0.1506 |
| **Set 3** | **DFA-PBE** | Default | 0.0566 |
| **Set 3** | **DFA-LDA** | Default | 0.0875 |

The density analysis for $\langle r^{-1} \rangle$ in **Set1** to **Set3** is represented in Table 3.19, 3.20, 3.21, and 3.22. The MAE for the different data sets is small, indicating small deviation for any KS density functional tested in different data sets. PZSIC PBE gives the least deviation from the CCSD(T) reference value for $\langle r^{-1} \rangle$ and this is true for **Set1**, **Set2a** and **Set2b**

The long-range moments of densities; $\langle r^1 \rangle$, $\langle r^2 \rangle$, and $\langle r^3 \rangle$ MAE could not be calculated as CCSD(T) reference values for those were not available, this is the same for $\langle r^{-2} \rangle$. The $\langle r^0 \rangle$ is the zero moments of the density which corresponds to the charge (atomic numbers) of the systems. The $\langle r^0 \rangle$ tested for all data sets were accurate and corresponded to the charge (atomic numbers) of the systems.

Data set **Set2a** and **Set2b** are hardly representative for most problems of $\langle r^n \rangle$ as there are too few electrons and too much dependence on charges and FOD's were more localized

in the core regions. Nonetheless, they were studied and MAE for $\langle r^{-1} \rangle$ is presented in table 3.20 and 3.21.

In **Set1**, DFA-PBE performs better than PZSIC-LSDA while PZSIC-PBE has the least deviation from the CCSD(T) reference value. But in **Set3**, DFA-PBE and DFA-LDA with the default NRLMOL basis set performed better than PZSIC PBE and PZSIC LSDA.

The radial distribution of the closed shell systems (Neon and Zinc); compared the performance of the density functional approximation DFA-PBE and the PZSIC-PBE, as represented by the graphs below fig 3.1 and fig 3.2.

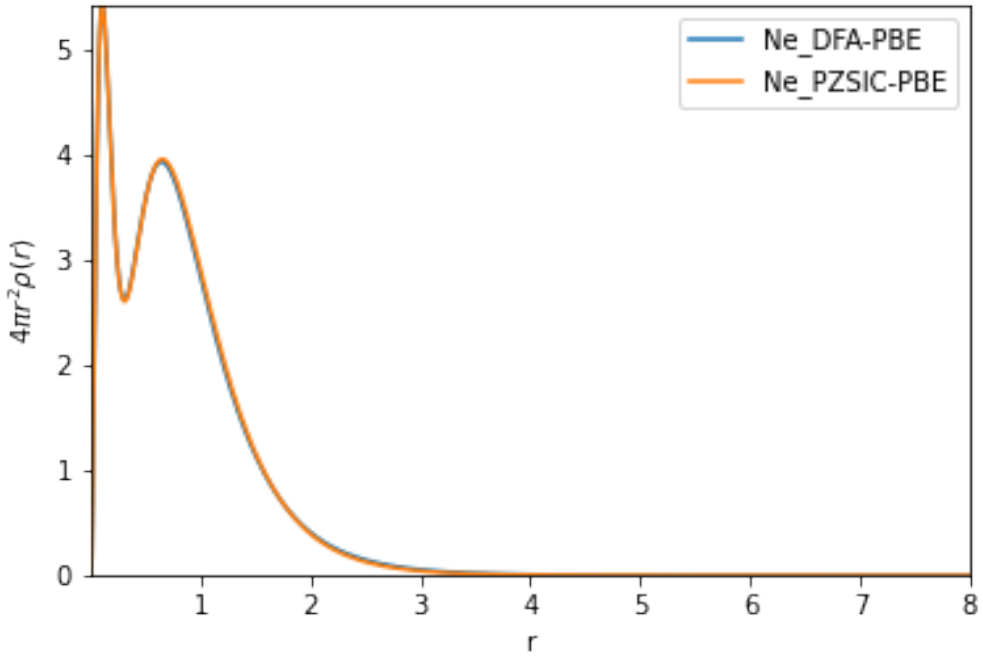


Figure 3.1: Radial Distribution of Ne with DFA-PBE and PZSIC-PBE using Default Basis

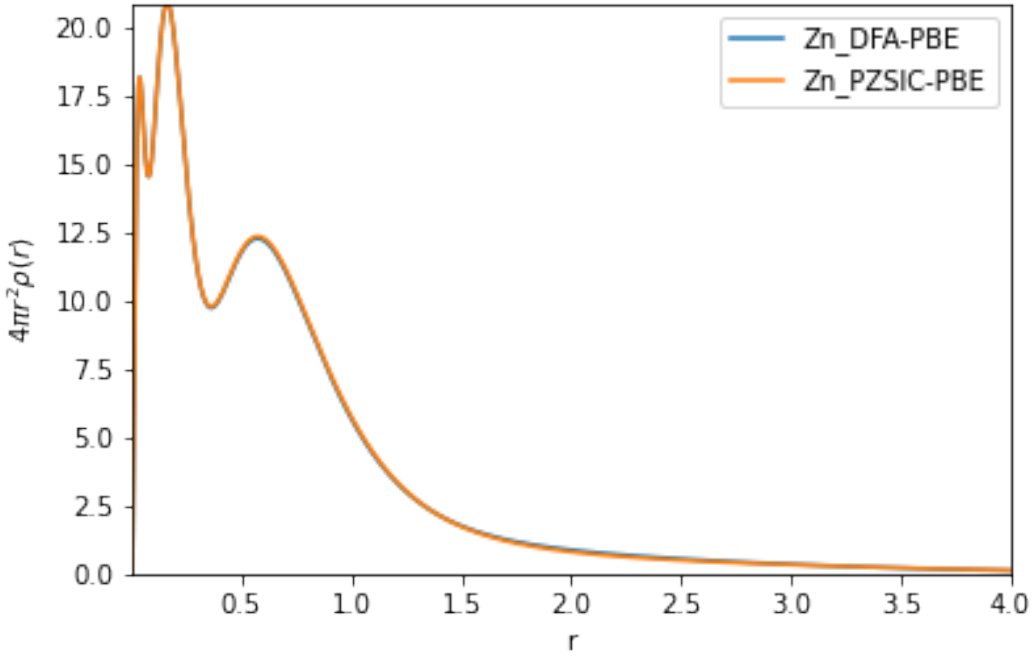


Figure 3.2: Radial Distribution of Zn with DFA-PBE and PZSIC-PBE using Default Basis

### 3.0.3 Summary

The accuracy of PZSIC and KS densities was investigated using the moment of densities from short-range to long-range regions. Three sets of data sets were investigated using LDA, PBE, PZSIC PBE, and PZSIC LSDA with different basis sets for all data set and functionals tested. The performance of the different functionals as represented in the radial distribution, indicated that the performance of different functionals were the same. The MAE of functionals with tested basis sets shows that basis sets has little or no influence on the accuracy of KS densities as the deviation of each basis sets and functionals were small in fraction of fractions. In Set1 through set2b, PZSIC-PBE with the least MAE shows the greatest accuracy while for transition metals in set3, DFA-PBE has the least MAE against the trend in set1 through set2b.

# Chapter 4

# Frozen Density Assessment of the Locally Scaled and Perdew-Zunger Self-interaction-Corrected Density Functional Approximations

A curious side effect of SIC-DFT calculations is the appearance of the so-called paradox of SIC, in which SIC tends to improve the accuracy of some energetic predictions, while degrading others. In particular, SIC-DFT tends to worsen equilibrium molecular properties of molecules and solids such as atomization energies and equilbrium geometries, and this degradation of accuracy only increases as a DFT calculation climbs Jacob's ladder and SIC is applied to semilocal and hybrid XC functionals. On the other hand, SIC-DFT performs well for nonequilibrium geometries such as stretched molecular bonds.

In 2019, Zope and coworkers were able to partially resolve the paradox by implementing a more selective SIC referred to as local-scaling SIC (LSIC) [19]. Fundamentally, LSIC corrects SIE in the same orbital wise fashion as PZSIC:

Zope and co-workers uses a pointwise iso-orbital indicator to identify the one-electron self-interaction regions in the many-electron system and to determine the magnitude of SIC in the many-electron regions[19, 43, 44].

$$E_{XC}^{LSIC-DFA} = E_{XC}^{DFA}[\rho,\rho] - \sum_i (U^{LSIC}[\rho_{i\sigma}] - E_{XC}^{LSIC}[\rho_{i\sigma,0}]) \tag{4.0.1}$$

However, the correction is scaled throughout space in such a way that it is only applied in regimes where it is actually needed[19].

$$U^{LSIC}[\rho_{i\sigma}] = \frac{1}{2}\iint dr_1 dr_2 \frac{(z_\sigma(r_1))^k \rho_{i\sigma}(r_1)\rho_{i\sigma}(r_2)}{r_{12}} \tag{4.0.2}$$

$$E_{XC}^{LSIC}[\rho_{i\sigma,0}] = \int dr (z_\sigma(r_1))^k \rho_{i\sigma}(r)\epsilon_{XC}^{DFA}([\rho_{i\sigma,0}], r) \tag{4.0.3}$$

The titular local-scaling comes in the form of the factor $z_\sigma$ which is defined as the ratio of the von Weizsacker kinetic energy density and the Kohn-Sham kinetic energy density[3, 43, 44, 45].

$$z_\sigma \equiv \frac{\tau_\sigma^w(r)}{\tau_\sigma(r)} \tag{4.0.4}$$

The noninteracting (Kohn-Sham) kinetic energy density is given as

$$\tau_\sigma(r) = \frac{1}{2}\sum_i \mid \bigtriangledown\psi_{i\sigma}(r) \mid^2 \tag{4.0.5}$$

and the von Weiszacker kinetic energy density is the single-orbital limit of $\tau_\sigma(r)$

$$\tau_\sigma^w(r) = \frac{\mid \bigtriangledown\rho_{i\sigma}(r) \mid^2}{8\rho_\sigma(r)} \tag{4.0.6}$$

By definition, $z_\sigma \epsilon [0, 1]$, where $z_\sigma = 0$ corresponds to uniform densities, and $z_\sigma = 1$ to one-electron densities. For this reason, $z_\sigma$ is called an iso-orbital indicator, as it detects single-orbital regions of the electron density. The exponent $k$ is a tunable parameter. In particular, $k = 0$ disables the scaling completely and recovers the PZSIC limit, while $k \to \infty$ reduces to a standard DFA by zeroing out SIC entirely. The simplest choice of $k = 1$ interpolates smoothly between the uniform density and one-electron limits[3].

### 4.0.1 Computational Details

The LSIC methods[43, 44, 45, 19, 3] using FLO's are implemented in the developmental version of the FLOSIC code[46, 45]. The FLOSIC code is based on the UTEP-NRLMOL code, which itself is a modernized version of legacy NRLMOL (FORTRAN 77) code[47] with many additional new capabilities[44]. We used the NRLMOL default basis set throughout our calculations.

In this work, we compare the performance of PZSIC and LSIC using frozen densities of different functionals and the Hatree Fock. FOD's from different functionals were optimized over the frozen densities for PZSIC and LSIC respectively and results were compared using different properties for PZSIC and LSIC. The self-consistency in the PZSIC calculations is obtained using Jacobi-like iterative procedure[43]. For LSIC calculations, we used the respective DFA densities and PZSIC FODs as a starting point.

The geometries used in our calculations are the same as in the respective databases and no further optimizations were performed. We used the SCF energy convergence criteria of $10^{-6}Eh$ for the total energy and an FOD force tolerance of $10^{-3}Eh$ per bohr for FOD optimizations in FLOSIC calculations[43]. To assess the performance of LSIC in comparison with PZSIC using frozen density calculations, we have calculated the atomization energies, barrier heights, etc.

### 4.0.2 Results And Discussion

We assessed the performance of LSIC and PZSIC using the wide array of electronic properties. We consider total energies, atomization energies, and the reaction barrier heights for molecules. The results are presented in this section.

#### Total Energies of Atoms

We compared the total atomic energies of the atoms Z = 1–18 against accurate non-relativistic values reported by Chakravorty et al [48]. The deviation of our calculation

from the reference value is represented in table 4.1 and also shown in fig 4.1

Table 4.1: MAE of atomic total energies (in $E_h$)

| Method | FOD's | Densities | MAE ($E_h$) |
|---|---|---|---|
| PZSIC | LSDA | HF | 0.373 |
| | LSDA | LSDA | 0.370 |
| | LSDA | PBE | 0.375 |
| | LSDA | SCAN | 0.374 |
| | PBE | HF | 0.166 |
| | PBE | LSDA | 0.171 |
| | PBE | PBE | 0.165 |
| | PBE | SCAN | 0.165 |
| LSIC | LSDA | HF | 0.042 |
| | LSDA | LSDA | 0.041 |
| | LSDA | PBE | 0.039 |
| | PBE | LSDA | 0.039 |
| | LSDA | SCAN | 0.039 |
| | SCAN | LSDA | 0.042 |
| DFA | | PBE | 0.083 |
| | | LSDA | 0.726 |
| | | SCAN | 0.019 |

Table 4.1 compared the total atomic energy from hydrogen through argon using LSIC and PZSIC methods, the deviation from the reference value in [48] were presented using the Mean Absolute Error (MAE). The MAE in PZSIC methods ranges from $0.165E_h$ to $0.375E_h$, this is comparable to the result obtained by Yamamoto et al in [44] where PZSIC-PBE, PZSIC-SCAN and PZSIC-LSDA have MAE's of $0.159, 0.147$ and $0.381E_h$ respectively. Yamamoto et al presented result for LSIC-LSDA pertubative, and LSIC-LSDA SCF, and SCF FOD optimized with MAE's of $0.041, 0.040$ and $0.040E_h$ respectively, and this is consistent with our results in table 4.1. Overall, LSIC methods predict accurately the total energies of atoms more than PZSIC methods, this might be part of the paradox of SIC as PZSIC might not accurately correct SIE. LSIC-LSDA optimized over PBE densities, LSIC-PBE optimized over LSDA densities, and LSIC-LSDA optimized over the SCAN densities, all have the least and same MAE of $0.039E_h$. These methods are sufficient to get good estimates of atomic energies.

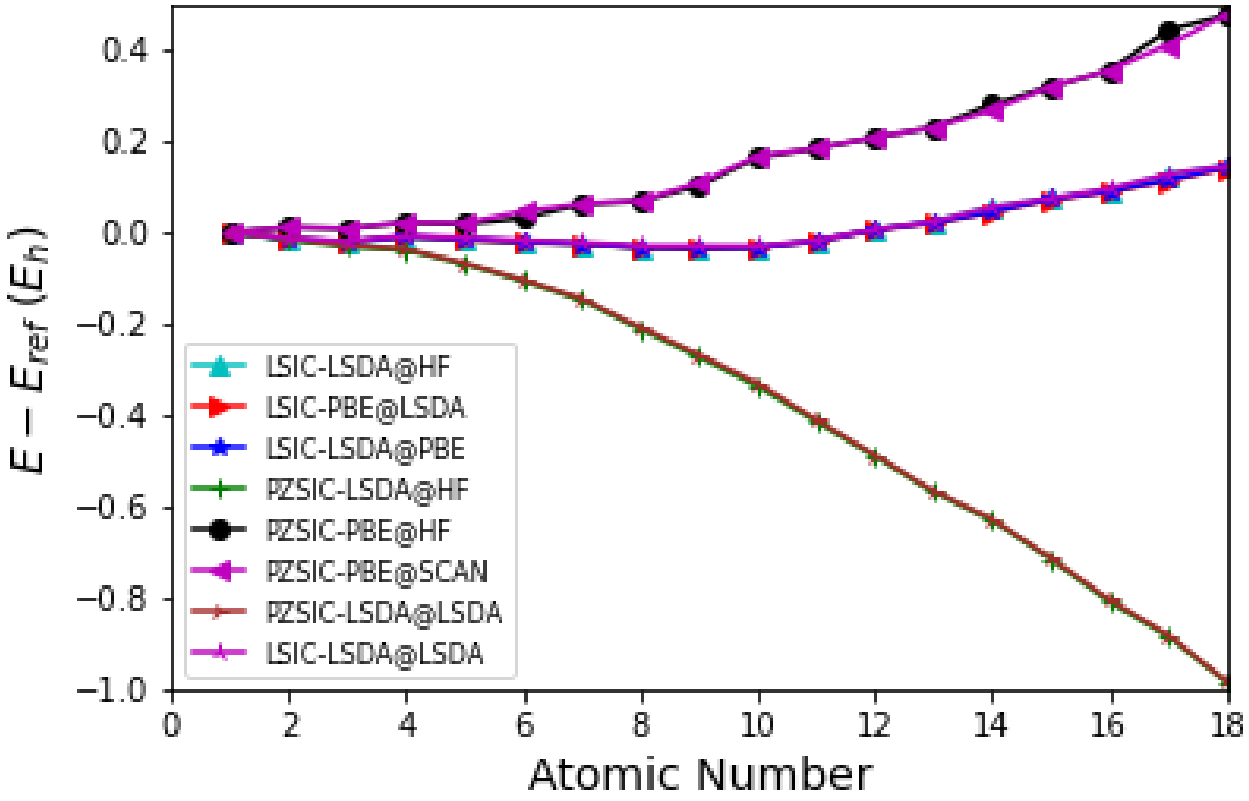


Figure 4.1: Total energies of atoms in $E_h$ compared against reference values

### Atomization Energies

We studied the performance of LSIC on atomization energies using the AE6 set[49] of molecules. The AE6 set is part of the Minnesota Database and is often used for benchmarking the performance of density functional approximations for atomization energies[44]. The AE6 set is composed of six molecules: $SiH_4$, $S_2$, $SiO$, $C_3H_4$ (propyne), $HCOCOH$ (glyoxal), and $C_4H_8$ (cyclobutane). The atomization energy $E_A$ is obtained as the energy difference of the sum of fragment atomic energies $E^i_{fragments}$ and the complex energy $E_{complex}$ as follows:

$$E_A = \sum_i E^i_{fragments} - E_{complex} \tag{4.0.7}$$

The MAE's are summarized in Table 4.2. Frozen density calculation with LSIC methods gave better performance than the PZSIC method. These results were compared with previously obtained results from the Electronic structure lab as reported in the publication reference [44]. Our results in table 4.2 is comparable with results in [44]. Yamamoto et al result indicated LSIC-LSDA, quasi-SCF method with MAE 6.57 $kcal/mol$, in table 4.2, LSDA density optimized over LSIC-LSDA FOD's performed better than other LSIC methods with MAE 9.67$kcal/mol$.

Table 4.2: MAE of the AE6 set of atomization energy

| Method | FOD's | Densities | MAE (Kcal/mol) |
|---|---|---|---|
| PZSIC | LSDA | HF | 57.46 |
| | LSDA | LSDA | 58.00 |
| | LSDA | PBE | 57.55 |
| | LSDA | SCAN | 81.14 |
| | PBE | HF | 19.23 |
| | PBE | LSDA | 21.33 |
| | PBE | PBE | 21.72 |
| | PBE | SCAN | 20.79 |
| LSIC | LSDA | HF | 10.06 |
| | LSDA | LSDA | 9.67 |
| | LSDA | PBE | 10.39 |
| | PBE | LSDA | 9.75 |
| | LSDA | SCAN | 28.23 |
| | SCAN | LSDA | 10.82 |
| DFA | | PBE | 13.43 |
| | | LSDA | 74.26 |
| | | SCAN | 2.85 |

**Barrier Heights**

An accurate description of chemical reaction barriers is challenging for DFAs since it involves the calculation of energies in non-equilibrium situations (i.e. at stretched bond distances). In most cases, the saddle point energies are underestimated since DFAs do not perform well for a non-equilibrium state that involves a stretched bond. This shortcoming of DFAs in a stretched bond case arises from SIE; when an electron is shared and stretched out, SIE incorrectly lowers the energy of transition states. SIC handles the stretched bond states accurately and provides a correct picture of chemical reaction paths. We studied the reaction barriers using the BH6 set of molecules for the LSIC and PZSIC method[43].

We used the BH6 set[49] of reactions to study the LSIC and PZSIC performance on barrier heights[44]. BH6 is a representative subset of the larger BH24[50] set consisting of three hydrogen transfer reactions

1. $OH + CH_4 \rightarrow CH_3 + H_2O$

2. $OH + H \rightarrow O + H_2$

3. $H + H_2S \rightarrow HS + H_2$

For each reaction, single point energies of the left- and right-hand side and saddle point of the reactions were calculated, and then forward and reverse barrier heights were computed[43, 44]. The barrier heights for the forward (f) and reverse (r) reactions were obtained by taking the energy differences of their corresponding reaction states[43]. The mean absolute errors (MAEs) of computed barrier heights are compared against the reference values[49] in table 4.3

Table 4.3: MAE of the BH6 set of barrier heights

| Method | FOD's | Densities | MAE (Kcal/mol) |
|---|---|---|---|
| PZSIC | LSDA | HF | 4.7 |
| | LSDA | LSDA | 14.02 |
| | LSDA | PBE | 3.23 |
| | LSDA | SCAN | 3.69 |
| | PBE | HF | 5.64 |
| | PBE | LSDA | 14.91 |
| | PBE | PBE | 5.60 |
| | PBE | SCAN | 5.44 |
| LSIC | LSDA | HF | 2.80 |
| | LSDA | LSDA | 7.16 |
| | LSDA | PBE | 1.36 |
| | PBE | LSDA | 1.41 |
| | LSDA | SCAN | 1.18 |
| | SCAN | LSDA | 1.37 |
| DFA | | PBE | 9.6 |
| | | LSDA | 17.6 |
| | | SCAN | 7.9 |

Most PZSIC calculations improve the barrier heights for semilocal functionals except for PZSIC-LSDA optimized with LSDA density, and PZSIC-PBE optimized with LSDA density have $14.02 kcal/mol$ and $14.91 kcal/mol$ as their respective MAE's. Application of LSIC raises barrier height and further reduces the MAE to as low as $1.18 kcal/mol$ for LSIC-LSDA optimized with SCAN density. We note that LSIC barrier heights are not necessarily between those predicted by DFA and PZSIC-DFA's since energy shifts vary for

reactants, products, and transition states. It is also noted that LSIC-LSDA FOD's with PBE density and LSIC-SCAN FOD optimized with LSDA density perform very similarly.

### 4.0.3 Summary

To summarize, in this work, we present frozen density calculations with LSIC and PZSIC methods. Performance assessment using standard benchmark database has been carried out on total energies, atomization energy, and barrier heights of reaction on standard data sets of molecules. Our results were compared with previously obtained results from the UTEP electronic structure laboratory. The result shows that LSIC performs better than PZSIC for all properties (total energies, atomization energies, and barrier heights) investigated.

# References


[1] W. Kohn and L. J. Sham, "Self-consistent equations including exchange and correlation effects," *Physical review*, vol. 140, no. 4A, p. A1133, 1965.

[2] L. J. Bartolotti and K. Flurchick, "An introduction to density functional theory," *Reviews in computational chemistry*, vol. 7, pp. 187–216, 2009.

[3] Z. J. Buschmann, *Two Developments for Efficient and Accurate Density Functional Theory Calculations*. PhD thesis, The University of Texas at El Paso, 2021.

[4] P. O. Ufondu, *Electron Binding Energy of Polar Molecules Using Fermi Lwdin Orbital Self Interaction Corrected Density Functional Scheme*. PhD thesis, The University of Texas at El Paso, 2019.

[5] A. Görling, "Density-functional theory beyond the hohenberg-kohn theorem," *Physical Review A*, vol. 59, no. 5, p. 3359, 1999.

[6] P. Hohenberg and W. Kohn, "Inhomogeneous electron gas phys. rev. 136," *B864*, 1964.

[7] A. J. Cohen, P. Mori-Sánchez, and W. Yang, "Challenges for density functional theory," *Chemical reviews*, vol. 112, no. 1, pp. 289–320, 2012.

[8] G. Oliver and J. Perdew, "Spin-density gradient expansion for the kinetic energy," *Physical Review A*, vol. 20, no. 2, p. 397, 1979.

[9] U. Von Barth and L. Hedin, "A local exchange-correlation potential for the spin polarized case. i," *Journal of Physics C: Solid State Physics*, vol. 5, no. 13, p. 1629, 1972.

[10] A. D. Becke, "A new mixing of hartree–fock and local density-functional theories," *The Journal of chemical physics*, vol. 98, no. 2, pp. 1372–1377, 1993.

[11] J. Sun, A. Ruzsinszky, and J. P. Perdew, "Strongly constrained and appropriately normed semilocal density functional," *Physical review letters*, vol. 115, no. 3, p. 036402, 2015.

[12] M. Probert, "Electronic structure: Basic theory and practical methods, by richard m. martin: Scope: graduate level textbook. level: theoretical materials scientists/condensed matter physicists/computational chemists," 2011.

[13] M. R. Pederson, "Fermi orbital derivatives in self-interaction corrected density functional theory: Applications to closed shell atoms," *The Journal of Chemical Physics*, vol. 142, no. 6, p. 064112, 2015.

[14] J. P. Perdew and A. Zunger, "Self-interaction correction to density-functional approximations for many-electron systems," *Physical Review B*, vol. 23, no. 10, p. 5048, 1981.

[15] Z.-h. Yang, M. R. Pederson, and J. P. Perdew, "Full self-consistency in the fermi-orbital self-interaction correction," *Physical Review A*, vol. 95, no. 5, p. 052505, 2017.

[16] M. R. Pederson, A. Ruzsinszky, and J. P. Perdew, "Communication: Self-interaction correction with unitary invariance in density functional theory," *The Journal of Chemical Physics*, vol. 140, no. 12, p. 121103, 2014.

[17] C. M. Diaz, P. Suryanarayana, Q. Xu, T. Baruah, J. E. Pask, and R. R. Zope, "Implementation of perdew–zunger self-interaction correction in real space using fermi–löwdin orbitals," *The Journal of Chemical Physics*, vol. 154, no. 8, p. 084112, 2021.

[18] M. R. Pederson, R. A. Heaton, and C. C. Lin, "Local-density hartree–fock theory of electronic states of molecules with self-interaction correction," *The Journal of chemical physics*, vol. 80, no. 5, pp. 1972–1975, 1984.

[19] R. R. Zope, Y. Yamamoto, C. M. Diaz, T. Baruah, J. E. Peralta, K. A. Jackson, B. Santra, and J. P. Perdew, "A step in the direction of resolving the paradox of

perdew-zunger self-interaction correction," *The Journal of Chemical Physics*, vol. 151, no. 21, p. 214108, 2019.

[20] P. Verma and R. J. Bartlett, "Increasing the applicability of density functional theory. iii. do consistent kohn-sham density functional methods exist?," *The Journal of Chemical Physics*, vol. 137, no. 13, p. 134102, 2012.

[21] Y. Shi and A. Wasserman, "Inverse kohn–sham density functional theory: progress and challenges," *The journal of physical chemistry letters*, vol. 12, no. 22, pp. 5308–5318, 2021.

[22] J. Wang, B. G. Johnson, R. J. Boyd, and L. A. Eriksson, "Electron densities of several small molecules as calculated from density functional theory," *The Journal of Physical Chemistry*, vol. 100, no. 15, pp. 6317–6324, 1996.

[23] M. E. Casida and D. Chong, "Recent advances in density functional methods," *Computational Chemistry: Reviews of Current Trends*, 1995.

[24] H. S. Yu, X. He, and D. G. Truhlar, "Mn15-l: A new local exchange-correlation functional for kohn–sham density functional theory with broad accuracy for atoms, molecules, and solids," *Journal of chemical theory and computation*, vol. 12, no. 3, pp. 1280–1293, 2016.

[25] S. Y. Haoyu, X. He, S. L. Li, and D. G. Truhlar, "Mn15: A kohn–sham global-hybrid exchange–correlation density functional with broad accuracy for multi-reference and single-reference systems and noncovalent interactions," *Chemical science*, vol. 7, no. 8, pp. 5032–5051, 2016.

[26] P. Verma and D. G. Truhlar, "Can kohn–sham density functional theory predict accurate charge distributions for both single-reference and multi-reference molecules?," *Physical Chemistry Chemical Physics*, vol. 19, no. 20, pp. 12898–12912, 2017.

[27] V. F. Lotrich, R. J. Bartlett, and I. Grabowski, "Intermolecular potential energy surfaces of weakly bound dimers computed from ab initio density functional theory: the right answer for the right reason," *Chemical physics letters*, vol. 405, no. 1-3, pp. 43–48, 2005.

[28] X. Xu, W. Zhang, M. Tang, and D. G. Truhlar, "Do practical standard coupled cluster calculations agree better than kohn–sham calculations with currently available functionals when compared to the best available experimental data for dissociation energies of bonds to 3 d transition metals?," *Journal of chemical theory and computation*, vol. 11, no. 5, pp. 2036–2052, 2015.

[29] R. J. Bartlett and D. S. Ranasinghe, "The power of exact conditions in electronic structure theory," *Chemical Physics Letters*, vol. 669, pp. 54–70, 2017.

[30] D. S. Ranasinghe, A. Perera, and R. J. Bartlett, "A note on the accuracy of ks-dft densities," *The Journal of Chemical Physics*, vol. 147, no. 20, p. 204103, 2017.

[31] M. G. Medvedev, I. S. Bushmarinov, J. Sun, J. P. Perdew, and K. A. Lyssenko, "Density functional theory is straying from the path toward the exact functional," *Science*, vol. 355, no. 6320, pp. 49–52, 2017.

[32] K. R. Brorsen, Y. Yang, M. V. Pak, and S. Hammes-Schiffer, "Is the accuracy of density functional theory for atomization energies and densities in bonding regions correlated?," *The journal of physical chemistry letters*, vol. 8, no. 9, pp. 2076–2081, 2017.

[33] G. D. Purvis III and R. J. Bartlett, "A full coupled-cluster singles and doubles model: The inclusion of disconnected triples," *The Journal of Chemical Physics*, vol. 76, no. 4, pp. 1910–1918, 1982.

[34] P. D. Mezei, G. I. Csonka, and M. Kallay, "Electron density errors and density-driven exchange-correlation energy errors in approximate density functional calculations," *Journal of chemical theory and computation*, vol. 13, no. 10, pp. 4753–4764, 2017.

[35] R. J. Boyd, J. Wang, and L. A. Eriksson, "The electron density as calculated from density functional theory," in *Recent Advances In Density Functional Methods: (Part I)*, pp. 369–401, World Scientific, 1995.

[36] A. D. Bochevarov and R. A. Friesner, "The densities produced by the density functional theory: Comparison to full configuration interaction," *The Journal of chemical physics*, vol. 128, no. 3, p. 034102, 2008.

[37] I. Grabowski, A. M. Teale, E. Fabiano, S. Śmiga, A. Buksztel, and F. D. Sala, "A density difference based analysis of orbital-dependent exchange-correlation functionals," *Molecular Physics*, vol. 112, no. 5-6, pp. 700–710, 2014.

[38] K. Raghavachari, G. W. Trucks, J. A. Pople, and M. Head-Gordon, "A fifth-order perturbation comparison of electron correlation theories," *Chemical Physics Letters*, vol. 157, no. 6, pp. 479–483, 1989.

[39] W. Kohn, "Nobel lecture: Electronic structure of matter—wave functions and density functionals," *Reviews of Modern Physics*, vol. 71, no. 5, p. 1253, 1999.

[40] I. V. Schweigert, V. F. Lotrich, and R. J. Bartlett, "Ab initio correlation functionals from second-order perturbation theory," *The Journal of chemical physics*, vol. 125, no. 10, p. 104108, 2006.

[41] P. Bhattarai, K. Wagle, C. Shahi, Y. Yamamoto, S. Romero, B. Santra, R. R. Zope, J. E. Peralta, K. A. Jackson, and J. P. Perdew, "A step in the direction of resolving the paradox of perdew–zunger self-interaction correction. ii. gauge consistency of the energy density at three levels of approximation," *The Journal of Chemical Physics*, vol. 152, no. 21, p. 214109, 2020.

[42] Y. Yamamoto, S. Romero, T. Baruah, and R. R. Zope, "Improvements in the orbitalwise scaling down of perdew–zunger self-interaction correction in many-electron regions," *The Journal of Chemical Physics*, vol. 152, no. 17, p. 174112, 2020.

[43] S. Romero, Y. Yamamoto, T. Baruah, and R. R. Zope, "Local self-interaction correction method with a simple scaling factor," *Physical Chemistry Chemical Physics*, vol. 23, no. 3, pp. 2406–2418, 2021.

[44] Y. Yamamoto, T. Baruah, P.-H. Chang, S. Romero, and R. R. Zope, "Self-consistent implementation of locally scaled self-interaction-correction method," *The Journal of Chemical Physics*, vol. 158, no. 6, 2023.

[45] P. Mishra, Y. Yamamoto, J. K. Johnson, K. A. Jackson, R. R. Zope, and T. Baruah, "Study of self-interaction-errors in barrier heights using locally scaled and perdew–zunger self-interaction methods," *The Journal of Chemical Physics*, vol. 156, no. 1, p. 014306, 2022.

[46] R. Zope, T. Baruah, and K. Jackson, "Flosic 0.2," *Based on the NRLMOL code of MR Pederson*.

[47] M. Pederson, D. Porezag, J. Kortus, and D. Patton, "Strategies for massively parallel local-orbital-based electronic structure methods," *Computer Simulation of Materials at Atomic Level*, pp. 197–218, 2000.

[48] S. J. Chakravorty, S. R. Gwaltney, E. R. Davidson, F. A. Parpia, and C. F. p Fischer, "Ground-state correlation energies for atomic ions with 3 to 18 electrons," *Physical Review A*, vol. 47, no. 5, p. 3649, 1993.

[49] B. J. Lynch and D. G. Truhlar, "Small representative benchmarks for thermochemical calculations," *The Journal of Physical Chemistry A*, vol. 107, no. 42, pp. 8996–8999, 2003.

[50] J. Zheng, Y. Zhao, and D. G. Truhlar, "Representative benchmark suites for barrier heights of diverse reaction types and assessment of electronic structure methods for thermochemical kinetics," *Journal of chemical theory and computation*, vol. 3, no. 2, pp. 569–582, 2007.

# Curriculum Vitae

Philip Adeniyi Oyedele was born in Iwo, Osun State, Nigeria. He completed his Bachelor of Science in Physics with a first-class degree from Ahmadu Bello University (ABU), which is a top ranked prestigious university of in Nigeria. He joined the University of Texas at El Paso in Fall, 2021 as a physics graduate student.

In the summer 2022, he interned with the Department of Physics at the University of Texas in Arlington as a Research Assistant under the supervision of Dr. Ben Jones where he worked on the Camera Read-out and Barium Tagging project.

He got the opportunity to work as a Teaching Assistant and became a member of the Electronic Structure research group under the supervision of Dr. Rajendra Zope in the Physics Department at the University of Texas at El Paso. His research is major on; Studies on Atomic and Molecular Properties Using Locally Scaled and Perdew-Zunger Self-Interaction Corrected Density Functional Approximations.

Upon graduation from UTEP with a Master of Science degree, he's determined to study further and hone his research skills in condensed matter physics by transiting to a Ph.D. program at the University of Texas at Arlington.

E-mail address: *paoyedele@miners.utep.edu, oyedelephilip@yahoo.com*